This figure is available in its entirety in the online version of the *Journal of Infectious Diseases*.

Figure 8. Frequency of $CD4^+CD25^+FoxP3^+$ cells.

$CD4^+CD25^+FoxP3^+$ cells was also decreased during lamivudine therapy. Moreover, the expression level of TLR2 on $CD4^+CD25^+$ cells gradually declined during entecavir therapy (Figure 7*G*).

Suppressive activity of T_{reg} cells. The suppressive activity of T_{reg} cells was analyzed by means of coincubation of unstained isolated T_{reg} cells and autologous $CD4^+CD25^-$ cells with CFSE staining. Ex vivo peripheral blood samples from 10 selected patients were analyzed before treatment, 3 months after the start of treatment, and 6 months after the start of treatment. The mean fluorescence intensity of the CFSE staining of the $CD4^+CD25^-$ cells was statistically significantly decreased at 6 months after the start of treatment ($P < .05$). These data indicate that the suppressive activity of T_{reg} cells was gradually decreased during entecavir treatment.

DISCUSSION

In this study, we have demonstrated that the levels of sHSP60 in patients with chronic hepatitis B were statistically significantly higher than those in patients with chronic hepatitis C. Moreover, the levels of sHSP60 were correlated with the HBV DNA levels but not with the ALT levels. On the other hand, the levels of sHSP70 were correlated with the ALT levels but not with the HBV DNA levels. This discrepancy in the correlation might be due to differences in the mechanism of heat shock protein production or secretion. The release of such heat shock proteins from cells is triggered by physical trauma and behavioral stress as well as by exposure to immunological danger signals [31, 32]. Stress protein release occurs both through physiological secretion mechanisms and during cell death by necrosis [33, 34]. HSP60 might be induced by the stress of HBV replication, because the levels of HSP60 were clearly correlated with the HBV DNA levels. On the other hand, HSP70 secretion might also be caused by cell death, because the levels of sHSP70 were correlated with the ALT levels. However, we should wait for more detailed studies about the HBV-specific induction of HSP60 to confirm this correlation. Extracellular stress proteins of the heat shock protein and glucose-regulated stress protein families, including HSP60, have powerful effects on the immune response [35]. Moreover, various kinds of immune cells such as macrophages, dendritic cells, $CD4^+$effector T cells, and T_{reg} cells are affected by heat shock proteins [28, 35]. Most recently, Cohen-Sfady et al [36] reported that HSP60 enhanced the activity of IL-10 secretion from B cells. This effect could support our findings of the immune-suppressive effect of HSP60. However, we can not draw conclusions about the whole effects of immune responses because the various kinds of immune cells might affect each other by means of cytokines, chemokines, stress-related proteins, and direct binding.

In this study, we focused on the effect of HSP60 on T_{reg} cell function by isolating T_{reg} cells, because many research groups had reported that the function and frequency of T_{reg} cells might be related to HBV replication. T_{reg} cells play an important role in the immune-hyporesponsiveness of patients with chronic hepatitis B. Previously, we demonstrated that the polarization of $CD4^+$ T cells was suppressed when the cells were stimulated with HBcAg in patients with chronic hepatitis B. T_{reg} cells are important cells in the suppression of the T helper 1 cell response by HBcAg, as demonstrated by the increased population of IL-10-secreting $CD4^+CD25^+$ cells. This indicates the presence of an inducible T_{reg} cell population, which is specific for HBcAg and produces IL-10, as well as a natural T_{reg} cell population in patients with chronic hepatitis B. Pretreatment with rHSP60 increased the frequency of HBcAg-specific IL-10-secreting $CD4^+CD25^+$ cells and enhanced the IL-10-secreting activity. These results indicate that pretreatment with rHSP60 might enhance the susceptibility of the HBcAg response and the function of IL-10 production by T_{reg} cells. These data might not imply that there was an expansion of HBcAg-specific T_{reg} cells as a result of the rHSP60 pretreatment, because the incubation phase was for only 16 h (4 h of pretreatment with rHSP60 plus 12 h of coincubation with HBcAg-presenting APCs). However, there is a possibility that continuous exposure to sHSP60 might induce an expansion of T_{reg} cells by enhancing the sensitivity of the expansion signal.

In this study, we found that the effect of HSP60 could be blocked by TLR2 neutralizing antibody but not by TLR4 neutralizing antibody. These data indicate that the effect of HSP60 could depend on TLR2. During entecavir therapy, not only the frequency of T_{reg} cells but also the serum levels of HSP60 and surface expression of TLR2 on T_{reg} cells gradually decreased. Therefore, we performed the suppression assay to detect the activity of T_{reg} cells by use of ex vivo isolated T_{reg} cells. The results of this suppression assay indicate that the reduction of the HBV DNA level could suppress the excessive activity of T_{reg} cells. In our previous study, the frequency and the function of HBV-specific cytotoxic T lymphocytes were partially recovered after therapy with nucleoside or nucleotide analogues [11]. The results clearly indicate that this restoration might be due to not only the reduction of HBV antigens but also the reduction of the frequency and function of T_{reg} cells.

On the basis of genomic analysis, 8 genotypes (A–H) of HBV have been defined, among which genotypes A, B, and especially C are prevalent in Japan [37–40]. Previous studies suggested that the clinical outcome of chronic hepatitis B was more severe in patients infected with genotype C, compared with those infected with genotype B [38, 39]. In this study, most of the

samples had HBV genotype C because of the high frequency of HBV genotype C infection in Japan. However, the expression levels of HSP60 were different among samples with the various genotypes in preliminary in vitro studies (data not shown). In addition, the expression patterns of chemokines in HBV-replicating Huh7 cells are apparently different among the various genotypes (Y. Kondo et al, unpublished data, May 2009). However, during entecavir treatment, the level of sHSP60 production in patients with genotype Bj HBV infection was quite similar to that in patients with genotype C HBV infection. We could not determine the relevance of the HBV genotypes and sHSP60 production levels because of the small numbers of genotype Bj–infected patients in this study.

In conclusion, we found that HSP60 was produced by HBV-replicating hepatocytes and determined the relevance of sHSP60 to T_{reg} cells functions, especially for IL-10-secreting activity. The understanding of the immunopathogensis of chronic hepatitis B could contribute to the development of novel kinds of immune therapy. Combination therapy with nucleoside or nucleotide analogues should be a reasonable method, because the suppression of HBV replication could reduce the excessive immune tolerance induced by T_{reg} cells.

References

1. Tiollais P, Pourcel C, Dejean A. The hepatitis B virus. Nature **1985**; 317:489–495.
2. Lai CL, Ratziu V, Yuen MF, Poynard T. Viral hepatitis B. Lancet **2003**; 362:2089–2094.
3. Kagi D, Ledermann B, Burki K, Zinkernagel RM, Hengartner H. Molecular mechanisms of lymphocyte-mediated cytotoxicity and their role in immunological protection and pathogenesis in vivo. Annu Rev Immunol **1996**; 14:207–232.
4. Peng G, Li S, Wu W, Sun Z, Chen Y, Chen Z. Circulating CD4+ CD25+ regulatory T cells correlate with chronic hepatitis B infection. Immunology **2008**; 123:57–65.
5. Barboza L, Salmen S, Goncalves L, et al. Antigen-induced regulatory T cells in HBV chronically infected patients. Virology **2007**; 368:41–49.
6. Kondo Y, Ueno Y, Shimosegawa T. Immunopathogenesis of hepatitis B persistent infection: implications for immunotherapeutic strategies. Clin J Gastroenterol **2009**; 2:71–79.
7. Xu D, Fu J, Jin L, et al. Circulating and liver resident CD4+CD25+ regulatory T cells actively influence the antiviral immune response and disease progression in patients with hepatitis B. J Immunol **2006**; 177: 739–747.
8. Manigold T, Racanelli V. T-cell regulation by CD4 regulatory T cells during hepatitis B and C virus infections: facts and controversies. Lancet Infect Dis **2007**; 7:804–813.
9. Kondo Y, Kobayashi K, Ueno Y, et al. Mechanism of T cell hyporesponsiveness to HBcAg is associated with regulatory T cells in chronic hepatitis B. World J Gastroenterol **2006**; 12:4310–4317.
10. Kondo Y, Kobayashi K, Asabe S, et al. Vigorous response of cytotoxic T lymphocytes associated with systemic activation of CD8 T lymphocytes in fulminant hepatitis B. Liver Int **2004**; 24:561–567.
11. Kondo Y, Asabe S, Kobayashi K, et al. Recovery of functional cytotoxic T lymphocytes during lamivudine therapy by acquiring multi-specificity. J Med Virol **2004**; 74:425–433.
12. Chisari FV, Ferrari C. Hepatitis B virus immunopathogenesis. Annu Rev Immunol **1995**; 13:29–60.
13. Reignat S, Webster GJ, Brown D, et al. Escaping high viral load exhaustion: CD8 cells with altered tetramer binding in chronic hepatitis B virus infection. J Exp Med **2002**; 195:1089–1101.
14. Suri-Payer E, Amar AZ, Thornton AM, Shevach EM. CD4+CD25+ T cells inhibit both the induction and effector function of autoreactive T cells and represent a unique lineage of immunoregulatory cells. J Immunol **1998**; 160:1212–1218.
15. Chen W, Jin W, Hardegen N, et al. Conversion of peripheral CD4+CD25− naive T cells to CD4+CD25+ regulatory T cells by TGF-beta induction of transcription factor Foxp3. J Exp Med **2003**; 198:1875–1886.
16. Hori S, Nomura T, Sakaguchi S. Control of regulatory T cell development by the transcription factor Foxp3. Science **2003**; 299:1057–1061.
17. Suvas S, Kumaraguru U, Pack CD, Lee S, Rouse BT. CD4+CD25+ T cells regulate virus-specific primary and memory CD8+ T cell responses. J Exp Med **2003**; 198:889–901.
18. Nakamura K, Kitani A, Fuss I, et al. TGF-beta 1 plays an important role in the mechanism of CD4+CD25+ regulatory T cell activity in both humans and mice. J Immunol **2004**; 172:834–842.
19. Zheng SG, Wang JH, Gray JD, Soucier H, Horwitz DA. Natural and induced CD4+CD25+ cells educate CD4+CD25− cells to develop suppressive activity: the role of IL-2, TGF-beta, and IL-10. J Immunol **2004**; 172:5213–5221.
20. Sundstedt A, O'Neill EJ, Nicolson KS, Wraith DC. Role for IL-10 in suppression mediated by peptide-induced regulatory T cells in vivo. J Immunol **2003**; 170:1240–1248.
21. Ulsenheimer A, Gerlach JT, Gruener NH, et al. Detection of functionally altered hepatitis C virus-specific CD4 T cells in acute and chronic hepatitis C. Hepatology **2003**; 37:1189–1198.
22. Marshall NA, Vickers MA, Barker RN. Regulatory T cells secreting IL-10 dominate the immune response to EBV latent membrane protein 1. J Immunol **2003**; 170:6183–6189.
23. Beilharz MW, Sammels LM, Paun A, et al. Timed ablation of regulatory CD4+ T cells can prevent murine AIDS progression. J Immunol **2004**; 172:4917–4925.
24. Wallin RP, Lundqvist A, More SH, von Bonin A, Kiessling R, Ljunggren HG. Heat-shock proteins as activators of the innate immune system. Trends Immunol **2002**; 23:130–135.
25. Raz I, Elias D, Avron A, Tamir M, Metzger M, Cohen IR. Beta-cell function in new-onset type 1 diabetes and immunomodulation with a heat-shock protein peptide (DiaPep277): a randomised, double-blind, phase II trial. Lancet **2001**; 358:1749–1753.
26. Hu W, Hasan A, Wilson A, et al. Experimental mucosal induction of uveitis with the 60-kDa heat shock protein-derived peptide 336–351. Eur J Immunol **1998**; 28:2444–2455.
27. Mor F, Cohen IR. T cells in the lesion of experimental autoimmune encephalomyelitis: enrichment for reactivities to myelin basic protein and to heat shock proteins. J Clin Invest **1992**; 90:2447–2455.
28. Zanin-Zhorov A, Cahalon L, Tal G, Margalit R, Lider O, Cohen IR. Heat shock protein 60 enhances CD4+ CD25+ regulatory T cell function via innate TLR2 signaling. J Clin Invest **2006**; 116:2022–2032.
29. Sugiyama M, Tanaka Y, Kato T, et al. Influence of hepatitis B virus genotypes on the intra- and extracellular expression of viral DNA and antigens. Hepatology **2006**; 44:915–924.
30. Inoue J, Takahashi M, Nishizawa T, et al. High prevalence of hepatitis delta virus infection detectable by enzyme immunoassay among apparently healthy individuals in Mongolia. J Med Virol **2005**; 76:333–340.
31. Lindquist S, Craig EA. The heat-shock proteins. Annu Rev Genet **1988**; 22:631–677.
32. Ellis RJ. The molecular chaperone concept. Semin Cell Biol **1990**; 1: 1–9.
33. Hightower LE, Guidon PT Jr. Selective release from cultured mammalian cells of heat-shock (stress) proteins that resemble glia-axon transfer proteins. J Cell Physiol **1989**; 138:257–266.
34. Mambula SS, Calderwood SK. Heat shock protein 70 is secreted from

tumor cells by a nonclassical pathway involving lysosomal endosomes. J Immunol **2006**; 177:7849–7857.
35. Calderwood SK, Mambula SS, Gray PJ Jr, Theriault JR. Extracellular heat shock proteins in cell signaling. FEBS Lett **2007**; 581:3689–3694.
36. Cohen-Sfady M, Pevsner-Fischer M, Margalit R, Cohen IR. Heat shock protein 60, via MyD88 innate signaling, protects B cells from apoptosis, spontaneous and induced. J Immunol **2009**; 183:890–896.
37. Mahmood S, Niiyama G, Kamei A, et al. Influence of viral load and genotype in the progression of hepatitis B-associated liver cirrhosis to hepatocellular carcinoma. Liver Int **2005**; 25:220–225.
38. Akuta N, Suzuki F, Kobayashi M, et al. Virological and biochemical relapse after discontinuation of lamivudine monotherapy for chronic hepatitis B in Japan: comparison with breakthrough hepatitis during long-term treatment. Intervirology **2005**; 48:174–182.
39. Kobayashi M, Suzuki F, Akuta N, et al. Response to long-term lamivudine treatment in patients infected with hepatitis B virus genotypes A, B, and C. J Med Virol **2006**; 78:1276–1283.
40. Tanaka Y, Mizokami M. Genetic diversity of hepatitis B virus as an important factor associated with differences in clinical outcomes. J Infect Dis **2007**; 195:1–4.

RNA Polymerase Activity and Specific RNA Structure Are Required for Efficient HCV Replication in Cultured Cells

Asako Murayama[1☯], Leiyun Weng[2☯], Tomoko Date[1], Daisuke Akazawa[1,3], Xiao Tian[2], Tetsuro Suzuki[1], Takanobu Kato[1], Yasuhito Tanaka[4], Masashi Mizokami[5], Takaji Wakita[1*], Tetsuya Toyoda[2*]

1 Department of Virology II, National Institute of Infectious Diseases, Tokyo, Japan, **2** Unit of Viral Genome Regulation, Key Laboratory of Molecular Virology & Immunology, Institute Pasteur of Shanghai, Chinese Academy of Sciences, Shanghai, People's Republic of China, **3** Pharmaceutical Research Lab, Toray Industries, Inc., Kanagawa, Japan, **4** Department of Clinical Molecular Informative Medicine, Nagoya City University Graduate School of Medical Sciences, Aichi, Japan, **5** Research Center for Hepatitis and Immunology, Kohnodai Hospital, International Medical Center of Japan, Chiba, Japan

Abstract

We have previously reported that the NS3 helicase (N3H) and NS5B-to-3′X (N5BX) regions are important for the efficient replication of hepatitis C virus (HCV) strain JFH-1 and viral production in HuH-7 cells. In the current study, we investigated the relationships between HCV genome replication, virus production, and the structure of N5BX. We found that the Q377R, A450S, S455N, R517K, and Y561F mutations in the NS5B region resulted in up-regulation of J6CF NS5B polymerase activity *in vitro*. However, the activation effects of these mutations on viral RNA replication and virus production with JFH-1 N3H appeared to differ. In the presence of the N3H region and 3′ untranslated region (UTR) of JFH-1, A450S, R517K, and Y561F together were sufficient to confer HCV genome replication activity and virus production ability to J6CF in cultured cells. Y561F was also involved in the kissing-loop interaction between SL3.2 in the NS5B region and SL2 in the 3′X region. We next analyzed the 3′ structure of HCV genome RNA. The shorter polyU/UC tracts of JFH-1 resulted in more efficient RNA replication than J6CF. Furthermore, 9458G in the JFH-1 variable region (VR) was responsible for RNA replication activity because of its RNA structures. In conclusion, N3H, high polymerase activity, enhanced kissing-loop interactions, and optimal viral RNA structure in the 3′UTR were required for J6CF replication in cultured cells.

Citation: Murayama A, Weng L, Date T, Akazawa D, Tian X, et al. (2010) RNA Polymerase Activity and Specific RNA Structure Are Required for Efficient HCV Replication in Cultured Cells. PLoS Pathog 6(4): e1000885. doi:10.1371/journal.ppat.1000885

Editor: Michael Gale Jr., University of Washington, United States of America

Received October 21, 2009; **Accepted** March 30, 2010; **Published** April 29, 2010

Funding: A.M. is supported by the Japan Health Sciences Foundation and Viral Hepatitis Research Foundation of Japan. This work was supported by grants from the Chinese Academy of Sciences (O514P51131 and KSCX1-YW-10-03), the Chinese 973 project (2009CB522504) and the Chinese National Key Project (2008ZX1000Z-14) to T.T., and a grant-in-aid for Scientific Research from the Japan Society for the Promotion of Science, from the Ministry of Health, Labor and Welfare of Japan, and from the Ministry of Education, Culture, Sports, Science and Technology and by the Research on Health Sciences Focusing on Drug Innovation from the Japan Health Sciences Foundation to T.W. The funders had no role in study design, data collection and analysis, decision to publish, or preparation of the manuscript.

Competing Interests: The authors have declared that no competing interests exist.

* E-mail: wakita@nih.go.jp (TW); ttoyoda@sibs.ac.cn (TT)

☯ These authors contributed equally to this work.

Introduction

Hepatitis C virus (HCV) contains a positive-stranded RNA genome and belongs to the *Flaviviridae* family [1]. Chronic HCV infection affects more than 130 million people worldwide [2]. The HCV RNA genome is approximately 9.6 kb in length and contains a long open reading frame that encodes a polyprotein of approximately 3,010 amino acids. This polyprotein is processed into at least 10 polypeptides by host and viral proteases [3,4]. The 5′-untranslated region (UTR) contains a highly conserved internal ribosome entry site (IRES) that is 341 nucleotides long [5]. The 3′UTR is known to contain a variable region (VR), a poly pyrimidine "U/C" (polyU/UC) tract, and a 98-base X-region (3′X tail) [6]. The second stem loop of the X region interacts with the NS5BSL3 cis-acting replication element (CRE) and may contribute to initiation of negative strand RNA synthesis [7].

JFH-1 belongs to genotype 2a and is the only strain that can efficiently replicate and produce virions in HuH-7 and HuH-7-derived cell lines [8,9,10]. When the structural protein-coding regions of the non-replicating HCV strains were fused to the non-structural protein-coding region and 3′UTR of JFH-1, replication was initiated and virions were produced in HuH-7-derived cells [10,11]. In order to analyze the mechanisms underlying the robust replication of JFH-1, we compared JFH-1 with J6CF. J6CF shares approximately 90% sequence homology with JFH-1 but does not replicate in HuH-7 cells. Analysis of JFH-1/J6CF chimeras demonstrated that the NS3 helicase-coding region (N3H) and the NS5B-to-3′X (N5BX) region of JFH-1 conferred replication activity to J6CF in HuH-7 cells [12]. Mutations in the N3H region are expected to affect helicase activity, while mutations in the NS5B-to-3′X region may affect polymerase and replication activity through secondary or higher order structures of the RNA. We have also previously reported that JFH-1-type mutations in the NS5B region enhanced genotype 1b RdRP activity *in vitro* [13]. Thus, JFH-1-type mutations in the NS5B region of J6CF are hypothesized to enhance J6CF RdRP activity. As mentioned above, the 3′UTR of the HCV genome consists of a VR, polyU/UC tracts of various lengths and a highly conserved 3′X tail. Deletion of the VR was reported to allow replication in both cultured cells [14] and in the chimpanzee [15]. The

Author Summary

Hepatitis C virus (HCV) is a major cause of chronic liver disease. Chronic HCV infection affects more than 130 million people worldwide. An efficient cell culture system is indispensable for HCV research and the development of antiviral strategies, including antiviral drugs and vaccines. Using one HCV strain, JFH-1, we have developed a novel cell culture system that, for the first time, has allowed for both the production of infectious HCV and the analysis of the HCV life cycle. To date, JFH-1 is the only HCV strain that replicates efficiently in cultured cells. Understanding the mechanisms underlying replication of JFH-1 in cultured cells is important and advantageous for the development of antiviral strategies. In the present study, we demonstrate that high polymerase activity, enhanced kissing-loop interactions between the NS5B and 3′X regions, and optimal viral RNA structure of the 3′ UTR are required for the efficient replication of JFH-1 and viral production in cultured cells. Our data provides information that will prove essential for the establishment of replication-competent variants of HCV strains that are currently replication incompetent in cultured cells. This study also contributes to a better understanding of the mechanisms underlying persistent HCV infections.

minimum length of polyU/UC tract required for replication has also been previously determined [14,16].

In the current study, we examined RNA polymerase activity and the RNA structures of the NS5B and 3′UTR that contribute to HCV replication, and determined the essential domains required for robust HCV RNA replication in cultured cells.

Materials and Methods

Cell culture

HuH-7 cells [17] and Huh-7.5.1 cells [9] were cultured at 37°C in Dulbecco's modified Eagle's medium containing 10% fetal bovine serum under 5% CO_2 conditions.

Construction of plasmids encoding a C-terminal 12xHis tagged HCV RdRP lacking 21 C-terminal amino acids

HCV JFH-1 and J6CF RdRP without the C-terminal 21 amino acid hydrophobic sequence were PCR amplified from pJFH1 [8] and pJ6CF (a kind gift from Jens Bukh) [15], respectively. Primer sequences for mutagenesis are listed in Table S1. Following digestion with *Xba*I and *Xho*I, DNA fragments were cloned into the *Nhe*I and *Xho*I sites of pET21b (Novagen, Madison, WI), resulting in pET21bHCVJFH-1RdRpwt and pET21bHCVJ6-CFRdRpwt. pET21bHCVJFH-1RdRpwt and pET21bHCVJ6-CFRdRpwt were then digested with *Xba*I and *Xho*I and the RdRP fragments cloned into the same restriction sites of pET28a, resulting in pET21(KM)JFH-1RdRpwt and pET21(KM)J6CFR-dRpwt, respectively.

Mutation analysis of J6CF and JFH-1 RdRP

JFH-1-type substitutions (S377R, A450S, S455N, R517K, and Y561F in the NS5B region; amino acid numbers are based on the AA relative numbering [18]) were introduced into J6CF RdRP and J6CF-like substitutions (S450A, N455S, K517R, F561Y, and F561I) and D318A were introduced into JFH-1 RdRP using the QuickChange II Site-Directed Mutagenesis Kit (Stratagene, La Jolla, CA). Primer sequences for mutagenesis are listed in Table S1. Sequences were confirmed by nucleotide sequencing.

Expression, purification, and *in vitro* transcription of HCV RdRP

pET21(KM)JFH-1RdRPwt, pET21(KM)J6CFRdRPwt, and their mutants were expressed with pGEX-HSP90α [13] in *Escherichia coli* Rosetta/pLysS (Novagen). RdRP was then purified as previously described [13], with the exception that protein induction was undertaken at 18°C for 4 h. *In vitro de novo* transcription was performed as described previously [13]. Briefly, following 30 min pre-incubation without ATP, CTP, or UTP, 0.1 μM HCV RdRP was incubated in 50 mM Tris/HCl (pH 8.0), 200 mM monopotassium glutamate, 3.5 mM $MnCl_2$, 1 mM DTT, 0.5 mM GTP, 50 μM ATP, 50 μM CTP, 5 μM [α-^{32}P]UTP, 0.02 μM RNA template (SL12-1S) and 100 U/ml human placental RNase inhibitor at 29°C for 90 min. [^{32}P]-RNA products were subjected to PAGE (6% gel, 8 M urea). The resulting autoradiograph was analyzed with a Typhoon trio plus image analyzer (GE Healthcare, Piscataway, NJ). The radio isotope count of 184 nt RNA product of each mutant RdRPs was measured and compared to that of JFH-1 RdRP wt in the same PAGE.

Subgenomic-replicon constructs

pSGR-J6/N3H+5BSLX-JFH1/Luc was constructed by replacement of the 5BSL-to-3′X fragment (9211 to 9678 of JFH-1) generated by PCR with the corresponding fragment of pSGR-J6/N3H+3′UTR-JFH1/Luc [12]. Constructs with substitutions in NS5B region were generated as follows; mutations were introduced by PCR-based mutagenesis and *Xho*I-*Xba*I-restricted fragments were exchanged with the corresponding fragment of pSGR-J6/N3H+5BSLX-JFH1/Luc or pSGR-J6/N3H+3′UTR-JFH1/Luc [12]. To generate the constructs used for the analyses of the 3′UTR, VR fragments (9415–9479 of JFH-1 and J6CF) or polyU/UC fragments (9480–9579 of JFH-1 and 9480–9606 of J6CF) were generated by PCR and replaced with the corresponding fragment of pSGR-J6/N3H+5BSLX-JFH1/Luc. To generate the constructs with substitutions in the VR or 3′SL2, mutations were introduced by PCR-based mutagenesis and *Sgr*AI-*Xba*I-restricted fragments were exchanged with the corresponding fragment of pSGR-J6/N3H+5BSLX-JFH1/Luc. Primer sequences for mutagenesis are listed in Table S1.

Full-length genomic HCV constructs

Plasmids used in the analysis of genomic RNA replication and core production were constructed from pJ6/N3H+N5BX-JFH1 [12] and pJ6CF [15]. pJ6/N3H+5BSLX-JFH1 was constructed by replacement of the corresponding sequence with the 5BSL-to-3′X fragment (9211 to 9678 of JFH-1) generated by PCR. pJ6/N3H+3′UTR-JFH1 was constructed by using the N3H region [*Cla*I (3929) - *Eco*T22I (5293)] and 3′UTR [*Stu*I (9415) - *Xba*I (9678)] of JFH-1 to replace the corresponding sequences of pJ6CF. Mutagenesis was performed as described above.

RNA synthesis and transfection

RNA synthesis and transfection were performed as described previously [8,12]. Briefly, plasmids were linearized with *Xba*I, treated with Mung Bean Nuclease (New England Biolabs, Ipswich, MA) and purified. Linearized, purified DNA was then used as a template for *in vitro* RNA synthesis using the MEGAscript T7 kit (Ambion, Austin, TX) in accordance with the manufacturer's instructions. Synthesized RNA was treated with DNase I (Ambion) followed by purification using ISOGEN-LS (Nippon Gene, Tokyo, Japan). The quality of the synthesized RNA was examined via agarose gel electrophoresis. Ten micrograms of *in vitro*-

synthesized RNA was used for each electroporation. Trypsinized HuH-7 cells or Huh-7.5.1 cells (3×10^6 cells) were washed with Opti-MEM I (Invitrogen, Carlsbad, CA) and resuspended in Cytomix buffer [19]. RNA was then combined with 400 µl of cell suspension and the mixture was transferred to an electroporation cuvette (Bio-Rad, Hercules, CA). The cells were then pulsed at 260 V and 950 µF using the Gene Pulser II apparatus (Bio-Rad). Transfected cells were immediately transferred to 6-well plates containing culture medium and incubated at 37°C under standard 5% CO_2 conditions.

Luciferase reporter assay

Luciferase activity of the JFH-1 subgenomic replicon and chimeras in HuH-7 cells were measured as described previously [12,20]. Briefly, 5 µg of transcribed RNA was transfected into 3×10^6 HuH-7 cells by electroporation. Transfected cells were immediately resuspended in culture medium and seeded into 6-well culture plates. Cells were then harvested at 4, 24, and 48 h after transfection and lysed with 200 µl of Cell Culture Lysis Reagent (Promega, Madison, WI). Debris was removed by centrifugation. Luciferase activity was quantified using a Lumat LB9507 luminometer (EG & G Berthold, Bad Wildbad, Germany) and a Luciferase Assay System (Promega). Assays were performed three times independently, with each value corrected for transfection efficiency as determined by measuring luciferase activity 4 h after transfection. Data are presented as relative light units (RLU).

Quantification of HCV core protein

To estimate the concentration of HCV core protein in the culture medium, we harvested supernatants at the indicated time points. The supernatant was then passed through a filter with a 0.22- µm pore size (Millipore, Bedford, MA) and subjected to the chemiluminescence enzyme immunoassay (Lumipulse II HCV core assay, Fujirebio, Tokyo, Japan) in accordance with the manufacturer's instructions.

Infection of cells with secreted HCV and determination of infectivity

Culture medium from RNA transfected cells was collected at 72 hours post-transfection. Huh7.5.1 cells were seeded at a density of 1×10^4 cells per well in poly-*D*-lysine coated 96-well plates (CORNING, Corning, NY). On the following day, the collected culture media were serially diluted and used for inoculation of the seeded cells, and the plates were incubated for another 3 days at 37°C. The cells were fixed in methanol for 15 min at −20°C, and the infected foci were visualized by immunofluorescence as described below.

Cells were blocked for 1 hour with BlockAce (Dainippon Sumitomo Pharma, Osaka, Japan), then washed with PBS, followed by incubation with anti-core antibody at 50 µg/ml in BlockAce. After incubation for 1 hour at room temperature, the cells were washed and incubated with a 1:400 dilution of AlexaFluor 488-conjugated anti-mouse IgG (Molecular Probes, Eugene, OR) in BlockAce. The cells were then washed and examined using fluorescence microscopy (Olympus, Tokyo, Japan). Infectivity was quantified by counting the infected foci and expressed as focus forming units per milliliter (ffu/ml).

Chemicals and radio isotope

Nucleotides were purchased from GE, [α-^{32}P]UTP from New England Nuclear (Boston, MA), and human placental RNase inhibitor and restriction enzymes from TaKaRa (Shiga, Japan).

Statistical analysis

Significant differences were evaluated using the Student's *t*-test. $p<0.05$ was considered significant.

RNA secondary structure prediction

RNA secondary structure prediction was performed using Mfold software [21].

Results

As we have reported previously, the NS3 helicase and the NS5B-to-3′X regions of JFH-1 are important to confer replication competence to J6CF, a replication-incompetent strain [12]. Of these two regions, NS5B-to-3′X of JFH-1 is the most important to replication-competence. The NS5B region encodes RdRP, and the JFH-1-version of this polymerase may have high activity and be crucial to replication-competence. The requirement of 3′UTR of JFH-1 suggested that the RNA structure in this region is important for efficient genome replication. To understand the mechanisms of efficient replication of JFH-1 in HuH-7 cells, we focused on the NS5B-to-3′X region because the NS3 helicase region of JFH-1 had relatively minor effects on replication of J6CF derivatives [12]. In order to identify the important protein domains within RdRP required for efficient virus replication, we compared the RNA polymerase activity of HCV J6CF RdRP to that of JFH-1 RdRP using three assays, *in vitro* transcription with purified RdRP, *in vivo* virus RNA replication, and *in vivo* virus production. To identify the important sequences or structures in the NS5B-to-3′X region involved in efficient replication, we analyzed the effect of sequence differences in this region on replication of the viral genome.

Comparison of RNA polymerase activity *in vitro*

By comparing the sequence of RdRP of JFH-1 (GenBank Accession No. AB047639), J6CF (AF177036), other 2a strains (AB047640 – 5, AY746460, AF238481 - 5, AF169002 -5), a 1a strain (H77: AF009606), and four 1b strains (Con1: AJ238799, AB080299, AY045702, M58335), we found 14 amino acids variants unique to JFH-1 RdRP (57T, 130P, 131Q, 150A, 377R, 405I, 435V, 450S, 455N, 474M, 479H, 517K, 561F and 571S). We focused on five JFH-1-type amino acid substitutions (Q377R, A450S, S455N, R517K, and Y561F) that have been shown to increase the polymerase activity of 1b RdRP [13]. We introduced these JFH-1-type amino acid substitutions into J6CF RdRP, individually and in combination, to test their effects on polymerase activity. We also tested a J6CF RdRP variant with a R517K substitution because it was included in the J6/N3H+5BSLX-JFH1 replicon (see below), although it did not enhance the polymerase activity of 1b RdRP *in vitro* [13].

The RdRPs of HCV JFH-1 and J6CF and mutant variants were purified as indicated in the Materials and Methods and Fig. S1A. The polymerase activity of wild-type (wt) and mutant RdRPs was measured using a *de novo* transcription system (Fig. 1 and Fig. S1B). The activity of J6CF RdRP was 7.0±0.6% of that of JFH-1. Similar to results seen with 1b RdRP substitution variants, the single amino acid substitutions Q377R, A450S, S455N, R517K, and Y561F resulted in increased polymerase activity of J6CF RdRP (25.5±1.5, 27.7±1.0, 53.1±0.9, 16.9±3.5 and 16.7±2.5% of JFH-1 RdRP wt, respectively). However, combining double and triple amino acid substitutions did not demonstrate any additive or synergistic effects on the *in vitro* polymerase activity (Fig. 1).

JFH-1 RdRP variants with individual J6CF-type amino acid substitutions, including R377Q, S450A, N455S, K517R, and F561Y, were also examined *in vitro*. With the exception of N455S,

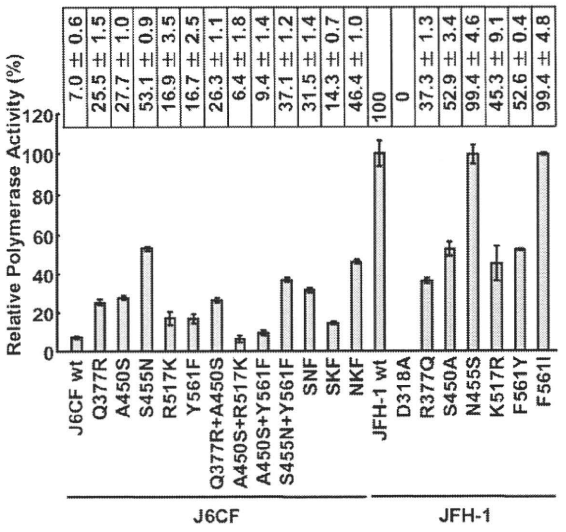

Figure 1. Relative HCV RNA polymerase activity of JFH-1 and J6CF wild-type and mutant RdRP. HCV RdRP activity was measured using the purified HCV RdRP (Fig. S1A) and the average RdRP activity and the standard deviation (error bar) relative to that of JFH-1 RdRP wt were calculated from three independent experiments (Representative gel images are shown in Fig. S1B). The relative activity values are presented above the graph. SNF, A450S+S455N+Y561F; SKF, A450S+R517K+Y561F; NKF, S455N+R517K+Y561F.
doi:10.1371/journal.ppat.1000885.g001

all other J6CF-type amino acid substitutions reduced the activity of JFH-1 RdRP, with levels ranging from 37.3 to 52.9% of the activity from wt JFH-1 RdRP (Fig. 1). The N455S variant maintained polymerase activity similar to that of JFH-1 wt. The JFH-1 D318A variant has a mutation in the active site of RdRP and showed no polymerase activity, confirming our *in vitro* transcription system.

JFH-1-type amino acid residues in the NS5B region restored the replication activity of the J6CF-based replicon

In order to test whether the JFH-1-type amino acids substitutions into the NS5B region of J6CF that enhanced polymerase activity *in vitro* enabled the replication of J6CF in cultured cells, we used the subgenomic J6CF replicon harboring the NS3 helicase region and 3′UTR of JFH-1 (J6/N3H+3′UTR-JFH1-Luc; Fig. 2A) as a reference construct. This replicon could replicate in cultured cells but exhibited less than 1% of the JFH-1 replication activity [12]. In order to test the effect of JFH-1 type amino acids on replication, we introduced the five substitutions that increased polymerase activity of J6CF RdRP *in vitro* (Q377R, A450S, S455N, R517K, and Y561F, see Fig. 2B) into the subgenomic replicon J6/N3H+3′UTR-JFH1-Luc and analyzed their effects on RNA replication. Among these JFH-1-type amino acids substitutions, Y561F was the most effective (23.2±3.5% of J6/N3H+N5BX-JFH1-Luc; Fig. 2C), while A450S, S455N, and R517K exhibited only a small effect on the replication activity (7.1±0.6%, 3.0±0.5%, and 5.5±1.0% of J6/N3H+N5BX-JFH1-Luc, respectively; Fig. 2C). The Q377R mutation demonstrated no effect on replication (Fig. 2C). We next tested the effects of Y561F in combination with each of the other substitutions. We found that A450S, S455N, and R517K mutations enhanced the replication activity of Y561F (59.1±6.1%, 43.9±6.6%, and 57.9±4.6% of J6/N3H+N5BX-JFH1-Luc, respectively; Fig. 2C). We also tested the effects of triple mutations and found that the replication activity of the SNF (A450S+S455N+Y561F) and SKF (A450S+R517K+Y561F) mutants demonstrated 86.8±6.0% and 112.2±7.9% replication activity of J6/N3H+N5BX-JFH1-Luc, respectively (Fig. 2C). In addition, we did not observe any significant differences between replicon activity of these mutants and that of J6/N3H+N5BX-JFH1-Luc. A combination of four mutations (SNKF; A450S+S455N+R517K+Y561F) resulted in similar activity as SKF (115.2±11.7% of J6/N3H+N5BX-JFH1-Luc; Fig. 2C). These results indicated that Y561F represented the most effective JFH-1-type mutation required for efficient replication, and that SKF and SNKF were sufficient to support replication activity equivalent to that of the replicon with the entire NS5B and 3′ UTR of JFH-1 (J6/N3H+N5BX-JFH1-Luc). The additive effects of the JFH-1-type NS5B substitutions on the replicon differed from results obtained with the *in vitro* polymerase activity assay.

Next, we examined whether these substitutions were sufficient for full-genome RNA replication and virus production. We used Huh-7.5.1 cells to assess virus production because Huh-7.5.1 is highly permissive for HCV propagation [9]. We found that J6/N3H+3′UTR-JFH1-Luc showed weak replication activity (Fig. 2C), and the core protein was not detectable in the culture medium of J6/N3H+3′UTR-JFH1-transfected cells (Fig. 3B). The constructs expressing A450S, S455N, or R517K substitution variants demonstrated only very low core levels in the supernatant, while the construct expressing the Y561F mutation underwent RNA replication and produced the core protein (Y561F; 15.5±3.0% of J6/N3H+N5BX-JFH1; Fig. 3B). Double mutants containing the Y561F mutation were found to produce greater amounts of core protein than the Y561F single mutant (A450S+Y561F, 57.4±3.3%; S455N+Y561F, 45.9±4.0%; and R517K+Y561F, 61.9±5.8% of J6/N3H+N5BX-JFH1; Fig. 3B). The triple mutant SNF (A450S+S455N+Y561F) produced more core protein than the double mutants (75.7±12.0% of J6/N3H+N5BX-JFH1; Fig. 3B). In addition, we observed that the core production from the SKF and SNKF mutant RNA-transfected cells was similar to the levels produced by J6/N3H+N5BX-JFH1 (111.5±8.8% and 119.0±5.1% of J6/N3H+N5BX-JFH1, respectively; Fig. 3B). We also measured infectivity of the supernatants from the mutant RNA-transfected cells at 72h after transfection (Fig. 3B). The levels of infectious titers correlated with the core levels among the tested constructs in this experiment. These results indicated that the SKF substitutions in the C-terminal region of NS5B were sufficient to elevate viral RNA replication and viral production.

Extra complementary sequence at the 5BSL3.2 kissing-loop interaction site of JFH-1 was essential for efficient replication

We observed a discrepancy between the *in vitro* RNA polymerase activity assay and the genome replication assay in the effects of the amino acid substitutions (Figs. 1 and 2C). Y561F was the most effective JFH-1-type amino acid substitution in the replication assay, while S455N was the most effective in the *in vitro* polymerase activity assay. As the kissing-loop interaction between 5BSL3.2 and 3′X are important for RNA replication and amino acid (aa) 561 encoding nucleotides are involved in the stem-loop 3.2 in the NS5B region (5BSL3.2) [7,16,22], we hypothesized that the cis-factor (genome structure) may also affect RNA replication in the cells. Thus, we constructed the subgenomic replicon J6/N3H+5BSLX-JFH1-Luc and the full genome construct J6/N3H+5BSLX-JFH1 that contained the NS3 helicase region and the 5BSL3-to-3′X region

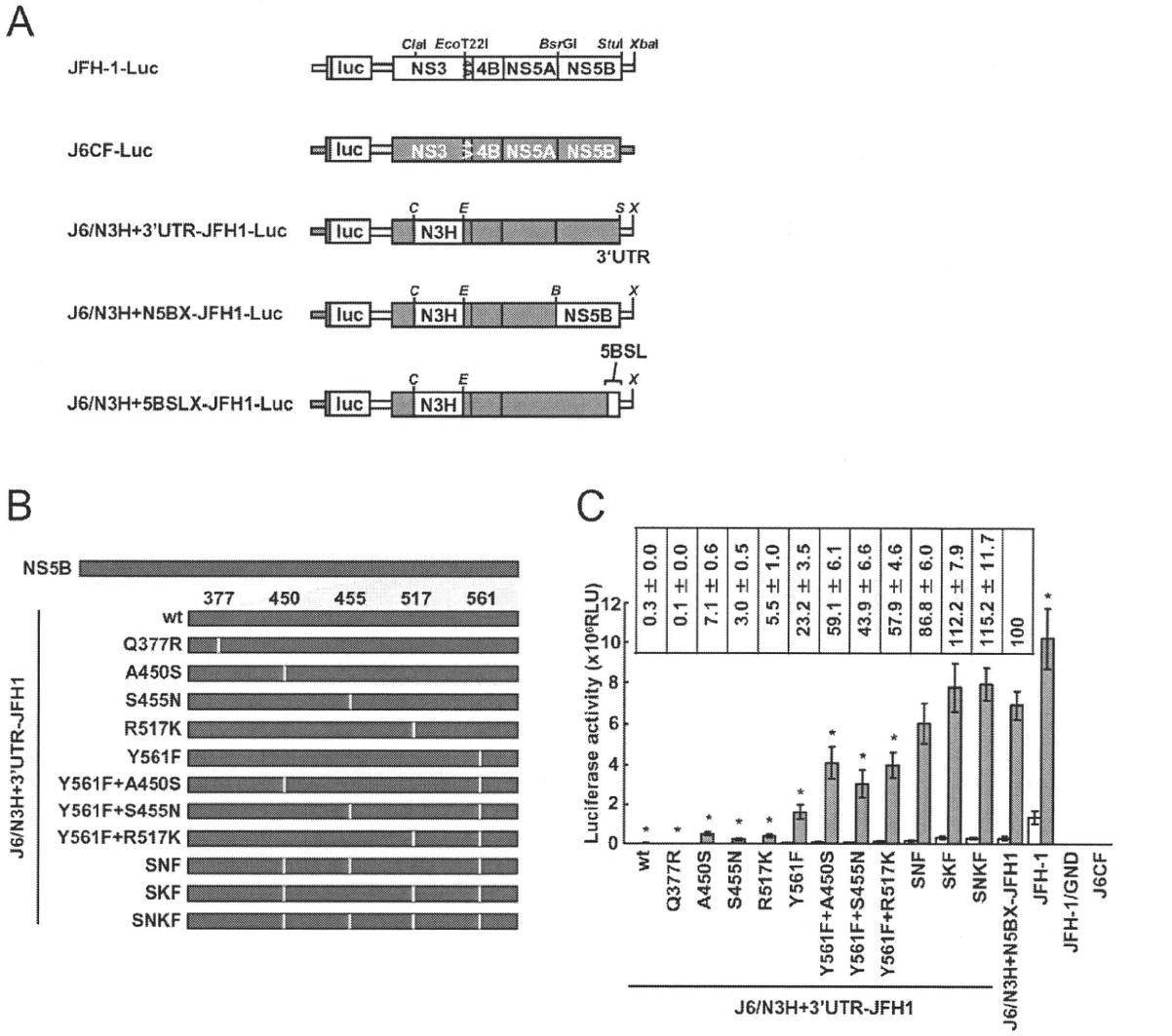

Figure 2. Luciferase activity of J6CF backbone replicons containing substitutions in the NS5B region. (A) Schematic structures of wt JFH-1 and J6CF constructs and the chimeric subgenomic replicons containing a J6CF backbone. The restriction enzyme recognition sites used for the construction of plasmids are indicated. *C*, *ClaI*; *E*, *Eco*T22I; *B*, *Bsr*GI; *S*, *StuI*; *X*, *XbaI*; wt, wild-type. (B) Schematic diagram of the mutations introduced into J6/N3H+3'UTR-JFH1-Luc and J6/N3H+3'UTR-JFH1. (C) Replication activity of J6CF-based replicons. Subgenomic RNA was synthesized *in vitro* from wild-type or chimeric replicon constructs. Transcribed subgenomic RNA (5 μg) was then electroporated into HuH-7 cells and the cells harvested at 4, 24, and 48 h after transfection. The harvested cells were lysed, and the luciferase activity in the cell lysates was measured. The assays were performed three times independently and the results expressed as luciferase activities (RLU). Each value was corrected for transfection efficiency as determined by measuring the luciferase activity 4 h after transfection. Data are presented as the mean ± standard deviation for luciferase activity at 24 h (white bars) and 48 h (gray bars) after transfection. Asterisks indicate significant differences relative to the replication activity of J6/N3H+N5BX-JFH1 ($p<0.05$) at 48 h and the values represent the relative values against J6/N3H+N5BX-JFH1 at 48 h after transfection. SNF, A450S+S455N+Y561F; SKF, A450S+R517K+Y561F; SNKF, A450S+ S455N+R517K+Y561F.

doi:10.1371/journal.ppat.1000885.g002

(nucleotide (nt) 9211 to 9678) of JFH-1 (Figs. 2A and 3A), and determined their replication activity and virus production level. As presented in Figure 4B, the J6/N3H+5BSLX-JFH1-Luc construct demonstrated similar replication activity to that of J6/N3H+N5BX-JFH1-Luc 48h post-transfection (92.9±7.5% of J6/N3H+N5BX-JFH1; Fig. 4B). Moreover, both J6/N3H+N5BX-JFH1 and J6/N3H+5BSLX-JFH1 released similar levels of core protein into the supernatant (Fig. 3B).

We next analyzed the effects of mutations in the J6/N3H+5BSLX-JFH1 construct. The 5BSL region of this construct contains three amino acid differences from J6CF (R517K, Y561F, and L571S). R517K and Y561F were important in the *in vitro* polymerase activity assay (Fig. 1). We did not assess aa 571 *in vitro* because it was deleted to purify HCV RdRP. The replication activities of J6/N3H+5BSLX-JFH1-Luc with K517R or F561Y were found to be 28±2.7% and 14±2.0% of J6/N3H+5BSLX-JFH1-Luc, respectively, confirming the importance of these JFH-1-type amino acids for replication (Fig. 4B). J6/N3H+5BSLX-JFH1-Luc with S571L revealed similar replicon activity as the J6/N3H+5BSLX-JFH1-Luc (108±7.8% of J6/N3H+5BSLX-JFH1

A

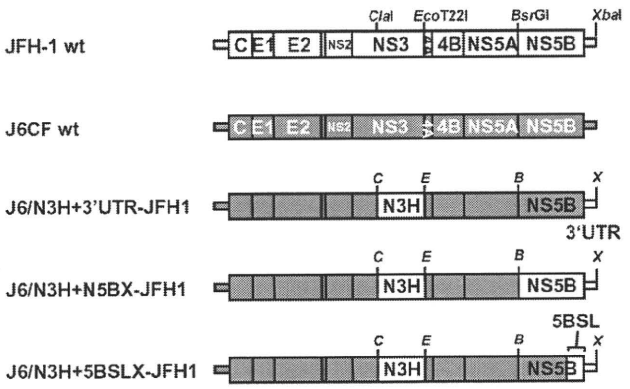

B

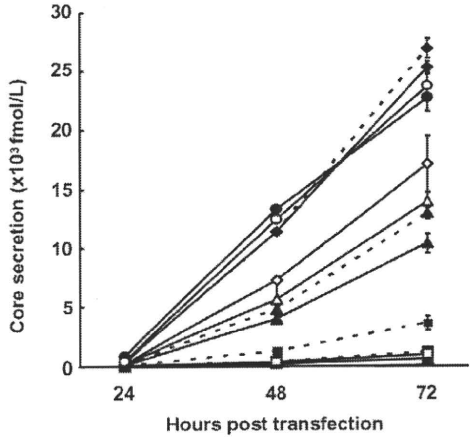

	Constructs	Core Secretion (%)	Infectivity (ffu/mL)
···◆···	SNKF	119.0 ± 5.1	$5.7x10^4$ ± $1.3x10^4$
—◆—	SKF	111.5 ± 8.8	$6.5x10^4$ ± $2.0x10^4$
—○—	J6/N3H+5BSLX-JFH1	104.7 ± 15.1	$5.8x10^4$ ± $4.7x10^3$
—●—	J6/N3H+N5BX-JFH1	100	$4.9x10^4$ ± $1.3x10^4$
—◇—	SNF	75.7 ± 12.0	$5.8x10^4$ ± $5.4x10^3$
—▲—	R517K+Y561F	61.9 ± 5.8	$4.3x10^4$ ± $5.8x10^3$
···★···	A450S+Y561F	57.4 ± 3.3	$2.6x10^4$ ± $6.9x10^3$
—▲—	S455N+Y561F	45.9 ± 4.0	$2.3x10^4$ ± $4.5x10^3$
···■···	Y561F	15.5 ± 3.0	$3.2x10^3$ ± $3.8x10^2$
—□—	R517K	4.2 ± 0.6	$7.0x10^1$ ± $1.0x10^1$
···□···	A450S	5.0 ± 0.1	$1.3x10^2$ ± $2.6x10^1$
—■—	S455N	2.7 ± 0.2	$1.4x10^2$ ± $3.1x10^1$
——	J6/N3H+3'UTR-JFH1	0.3 ± 0.1	$5.0x10^{-1}$ ± $0.0x10^0$

Figure 3. Analysis of transient replication of genomic chimeric HCV RNA. (A) The structure of full-length chimeric HCV RNA. Each chimeric full-length construct was prepared by the replacement of the indicated restricted fragments. The restriction enzyme recognition sites used for the plasmid constructions are indicated. *C*, *ClaI*; *E*, *Eco*T22I; *B*, *Bsr*GI; *S*, *StuI*; *X*, *XbaI*; wt, wild-type. (B) HCV core protein production in the culture medium from RNA-transfected cells. Transcribed wild-type or chimeric full-length HCV RNA (10 μg) was transfected into Huh-7.5.1 cells. Culture medium was harvested at 4, 24, 48, and 72 h after transfection. The amount of core protein in the harvested culture medium was measured using a HCV core chemiluminescence enzyme immunoassay (Lumipulse II HCV core assay). The assays were performed three times independently, and the data are presented as the mean ± standard deviation. Values in the right panel represent the relative core values against J6/N3H+N5BX-JFH1 at 72 h after transfection and infectious titers of the media from chimeric HCV RNA-transfected cells at 72h after transfection determined using Huh7.5.1 cells. SNF, A450S+S455N+Y561F; SKF, A450S+R517K+Y561F; SNKF, A450S+ S455N+R517K+Y561F.
doi:10.1371/journal.ppat.1000885.g003

wt; Fig. 4B). These results indicated the importance of 517K and 561F but not 571F in the 5BSL region of JFH-1 in efficient RNA replication. The codon encoding aa 561 possibly affects RNA structure, as it is located in the loop of stem-loop 3.2 in NS5B (5BSL3.2) and overlaps sequences important to the kissing-loop interaction with the stem loop 2 of the 3′X region (3′X SL2) [22]. Although we demonstrated that aa 561F was more effective than 561Y in RdRP activity *in vitro* (Fig. 1), it remains possible that the nucleotide mutation located at the codon of aa 561 affected the RNA structure and genome replication, as the replication activity of J6/N3H+3′UTR-JFH1-Luc with Y561F was the highest of all the clones with JFH-1 type single amino acids in the NS5B region (Fig. 2C). To investigate the effects of these mutations on RNA structure, we made mutants with nucleotide substitutions at the codon of aa 561 (Fig. 4F). The codon encoding aa 561 was UUU (Phe) for JFH-1 and UAU (Tyr) for J6CF. The third base of the codon overlaps with the kissing sequence [22]. In order to maintain the 5BSL3.2 stem loop structure and the kissing interaction between 5BSL3.2 and 3′X SL2, the third base should be U (nt 9349 of JFH-1). JFH-1 may exhibit additional interactions between 9348U of 5BSL3.2 and 9619A of 3′X SL2 to enhance kissing-loop interaction. To assess this hypothesis, we fixed the second base (9348) as U, and the first base (9347) was altered from U to A, G or C. The G and C substitutions were predicted to disrupt the important loop structure of 5BSL3.2 using Mfold and considered to affect replication activity. We next investigated the effects of U to A substitution (AUU, F561I) in an *in vitro* assay. F561I was introduced into JFH-1 RdRP and its RdRP activity was 99.4±4.8% of the wt, demonstrating that an F to I mutation did not affect polymerase activity (Fig. 1). We also examined the effects of the F561I mutation on RNA replication in the cells, and it revealed that it had similar replication activity as the wt,

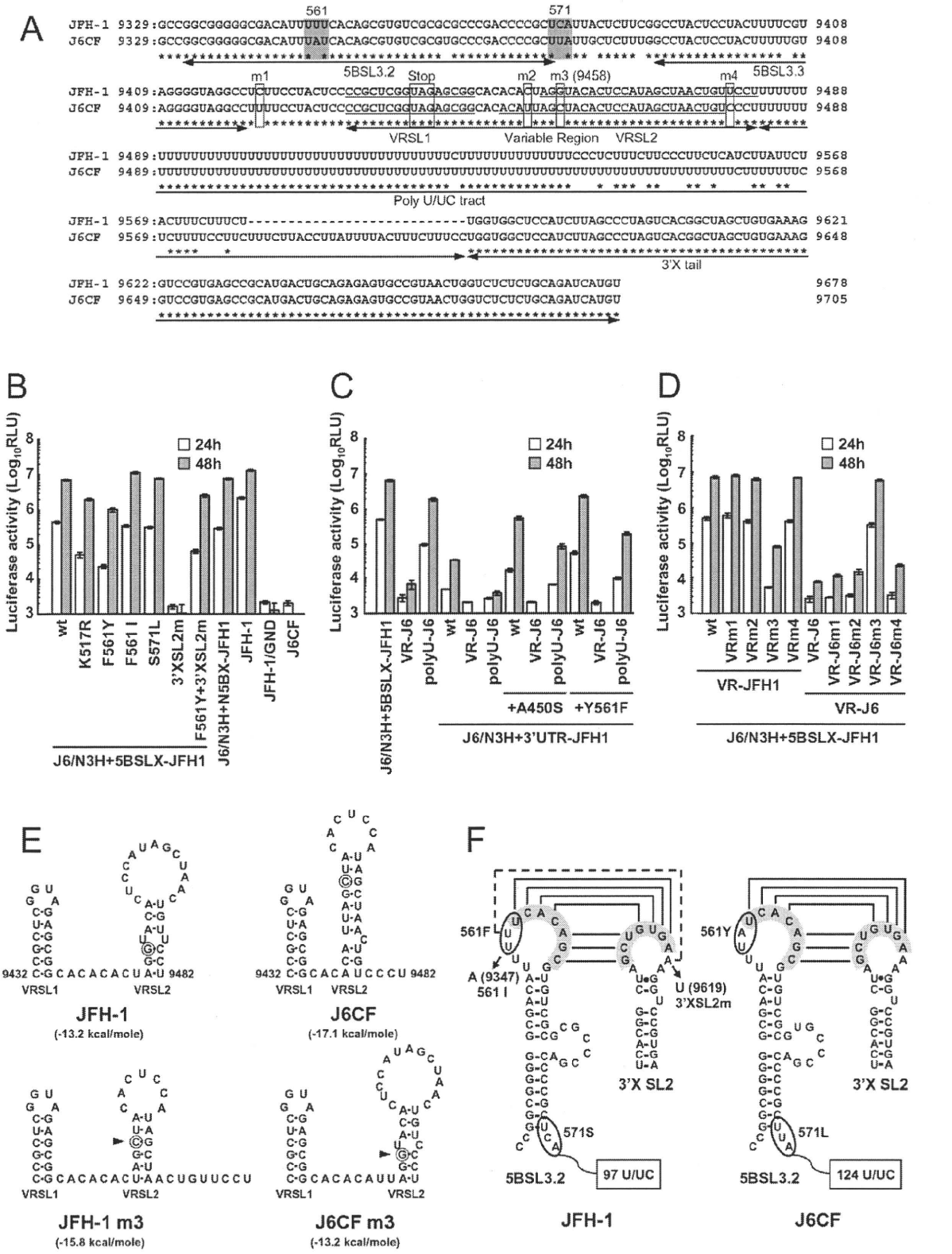
A
561
571
JFH-1 9329:GCCGGCGGGGGCGACAUUUUUCACAGCGUGUCGCGCGCCCGACCCCGCUCAUUACUCUUCGGCCUACUCCUACUUUUCGU 9408
J6CF 9329:GCCGGCGGGGGCGACAUUUAUCACAGCGUGUCGCGUGCCCGACCCCGCUUAUUGCUCUUUGGCCUACUCCUACUUUUUGU 9408
5BSL3.2
Stop
m1
m2
m3 (9458)
m4
5BSL3.3
JFH-1 9409:AGGGGUAGGCCUCUUCCUACUCCCCGCUCGGUAGAGCGGCACACACUAGGUACACUCCAUAGCUAACUGUUCCUUUUUUU 9488
J6CF 9409:AGGGGUAGGCCUUUUCCUACUCCCCGCUCGGUAGAGCGGCACACAUUAGCUACACUCCAUAGCUAACUGUCCCUUUUUUU 9488
VRSL1
Variable Region
VRSL2
JFH-1 9489:UUUUUUUUUUUUUUUUUUUUUUUUUUUUUUUUUUUUUUUUCUUUUUUUUUUUUUUCCCUCUUUCUUCCCUUCUCAUCUUAUUCU 9568
J6CF 9489:UUUUUUUUUUUUUUUUUUUUUUUUUUUUUUUUUUUUUUUUUUUUUUUUUUUUUUUUUUUUUUUUUUUUUUUUUUUUUUUUUUC 9568
Poly U/UC tract
JFH-1 9569:ACUUUCUUUCU----------UGGUGGCUCCAUCUUAGCCCUAGUCACGGCUAGCUGUGAAAG 9621
J6CF 9569:UCUUUUCCUUCUUUCUUACCUUAUUUUACUUUCUUUCCUGGUGGCUCCAUCUUAGCCCUAGUCACGGCUAGCUGUGAAAG 9648
3'X tail
JFH-1 9622:GUCCGUGAGCCGCAUGACUGCAGAGAGUGCCGUAACUGGUCUCUCUGCAGAUCAUGU 9678
J6CF 9649:GUCCGUGAGCCGCAUGACUGCAGAGAGUGCCGUAACUGGUCUCUCUGCAGAUCAUGU 9705
B
Luciferase activity (Log10RLU)
24h
48h
wt
K517R
F561Y
F561 I
S571L
3'XSL2m
F561Y+3'XSL2m
J6/N3H+N5BX-JFH1
JFH-1
JFH-1/GND
J6CF
J6/N3H+5BSLX-JFH1
C
Luciferase activity (Log10RLU)
24h
48h
J6/N3H+5BSLX-JFH1
VR-J6
polyU-J6
wt
VR-J6
polyU-J6
wt
VR-J6
polyU-J6
wt
VR-J6
polyU-J6
+A450S
+Y561F
J6/N3H+3'UTR-JFH1
D
Luciferase activity (Log10RLU)
24h
48h
wt
VRm1
VRm2
VRm3
VRm4
VR-J6
VR-J6m1
VR-J6m2
VR-J6m3
VR-J6m4
VR-JFH1
VR-J6
J6/N3H+5BSLX-JFH1
E
JFH-1
(-13.2 kcal/mole)
J6CF
(-17.1 kcal/mole)
JFH-1 m3
(-15.8 kcal/mole)
J6CF m3
(-13.2 kcal/mole)
VRSL1
VRSL2
F
561F
A (9347)
561 I
U (9619)
3'XSL2m
3'X SL2
571S
5BSL3.2
97 U/UC
JFH-1
561Y
571L
124 U/UC
J6CF

Figure 4. Replication activity of J6CF-based replicons containing variants or substitutions. (A) Comparison of the nucleotide sequence of 5BSL3.2 to 3′X of JFH-1 and J6CF. Boxes indicate nucleotide differences in VR and stop codon. Shaded boxes indicate non-synonymous variants in this region. 5BSL3.2, 5BSL3.3, Variable Region (VR), Poly U/UC tract, and 3′X tail are indicated by double-headed arrows in the figure. Stem-loop structures of VR (VRSL1 and VRSL2) are underlined. Asterisk; conserved nucleotides between JFH-1 and J6CF. (B, C, D) Replication activity of J6CF-based replicons. Five micrograms of *in vitro* synthesized RNA was electroporated into HuH-7 cells and the cells were harvested at 4, 24, and 48 h after transfection. The harvested cells were then lysed, and the luciferase activity in the cell lysates was measured. The assays were performed three times independently, and the results were expressed as luciferase activities (RLU). Data are presented as the mean ± standard deviation for luciferase activity at 24 h (white bars) and 48 h (gray bars) after transfection. (E) The predicted secondary structure of the VR. The RNA secondary structures of JFH-1, JFH-1 m3, J6CF, and J6CF m3 were predicated by Mfold. The stem-loop structure 1 (VRSL1) and 2 (VRSL2) are indicated. Nucleotide 9458 is circled and the mutated nucleotides are indicated by arrowheads. (F) Schematic structures of the 5BSL3.2 and X tail. The predicted stem loop structure of 5BSL3.2 and SL2 of 3′X of JFH-1 and J6CF strains are indicated. The sequences forming kissing interaction with 3′X SL2 [22] are shaded. Codons encoding aa 561 and 571 are circled and the mutated sequences are indicated. The reported kissing-loop interactions are indicated by the connecting lines. The predicted interaction of the JFH-1 strain is indicated by the dotted connecting line.
doi:10.1371/journal.ppat.1000885.g004

confirming that this mutation exhibited no effect on RNA replication in cultured cells (Fig. 4B). These results demonstrated that both Phe and Ile could be substituted at aa 561 and revealed the importance of the precise RNA structure of this region. Finally, we introduced an A to U mutation at nt 9619 in the 3′X SL2 that was complementary to the second base of the codon encoding 561F (9348) to alter the kissing-loop interaction (Fig. 4F; 3′XSL2m). We observed a significant reduction in 3′XSL2m replication activity (Fig. 4B; 3′XSL2m). However, when 3′XSL2m was combined with the F561Y mutation that was expected to recover the kissing-loop interaction, replicon activity was restored (Fig. 4B; F561Y+3′XSL2m). These results indicated that the extra complementary sequence at the kissing-loop interaction site of 5BSL3.2 was important for the efficient RNA replication of JFH-1. The extra complementary sequence may enhance the kissing loop interactions. We also tested the effect of the Y561F substitution on replicons of other genotypes, H77S (GT1a) and HCV-N (GT1b). While the Y561F substitution increased replication activity in both genotype 1 strains (Text S1 and Fig. S3), the Y561F effect on the genotype 1 strains was much smaller than its corresponding effect on J6CF.

A shorter poly U/UC sequence in the JFH-1 strain favored replication

We next compared the sequences of the poly U/UC tracts of the 3′UTRs of JFH-1 and J6CF. The poly U/UC tract of JFH-1 was 27 nucleotides shorter than that of J6CF (Figs. 4A and F). The polyU stretch of the pJ6CF plasmid that we used was six nucleotides shorter than that of the original J6CF sequence reported ([15], GenBank: AF177036). In order to analyze the effects of poly U/UC length on HCV replication, the poly U/UC region of J6/N3H+5BSLX-JFH1-Luc was replaced with that of J6CF and was designated as polyU-J6. The replicon activity of J6/N3H+5BSLX-JFH1-Luc with polyU-J6 was approximately four times lower than that of the J6/N3H+5BSLX-JFH1-Luc (Fig. 4C). This result showed that longer polyU/UC region lengths of J6CF were not favorable for efficient replication.

JFH-1 type structure of the variable region was advantageous for efficient replication

When we compared the VR sequences of the 3′UTRs of JFH-1 and J6CF, we found that four nucleotides are different between the VRs of JFH-1 and J6CF and that substitution of the VR from JFH-1 with that of J6CF of J6/N3H+5BSLX-JFH1 resulted in a 1000-fold decrease in replication activity (Fig. 4C, VR-J6). Mfold analysis of predicted RNA secondary structure of the VR in JFH-1 and J6CF suggests that there are two stem-loop structures in the VR. The first stem loop (VRSL1) structure is identical in JFH-1 and J6CF, but the loop of the second stem-loop (VRSL2) is larger in JFH-1 than in J6CF (Fig. 4E). Analysis of the effects of these nucleotide mutations on RNA structure revealed that only the third mutation (m3 at 9458 in Fig. 4A) is predicted to alter the structure of VRSL2 (Fig. 4E). The m3 G substitution into J6CF VR generated a predicted structure identical to that of JFH-1 VRSL2 resulting in identical VR structures (Fig. 4E). The m3 C substitution altered the structure of JFH-1 VR to the J6CF type (Fig. 4E). Substitutions of other nucleotides did not change the predicted structures (Data not shown). We then analyzed the effects of the mutations on replication activity. The m3 C substitution in JFH-1 VR was found to reduce replication activity 100-fold of the J6/N3H+5BSLX-JFH1-Luc (Fig. 4D; VRm3), whereas other substitutions (Fig. 4A; m1, m2 and m4) did not reduce replication activity at all (Fig. 4D; VRm1, VRm2 and VRm4). In contrast, the construct containing the J6CF VR with m3 G substitution completely restored replication activity (Fig. 4D; VR-J6m3). Other JFH-1 type nucleotide did not restore replication activity (Fig. 4D; VR-J6m1, VR-J6m2 and VR-J6m4). These results were in agreement with the stem-loop structure prediction of VR (Fig. 4E), demonstrating that the JFH-1 VR increased RNA replication. These results suggested the importance of VR secondary structure. Next, we tested if the effect of VR of JFH-1 was restricted to NS5B of JFH-1 or not. We constructed replicons with NS5B of J6CF and tested the effect on replication. The replication activities of the replicon with entire NS5B of J6CF (J6/N3H+3′UTR-JFH1), J6/N3H+3′UTR-JFH1 with A450S or Y561F (J6/N3H+3′UTR-JFH1+A450S, J6/N3H+3′UTR-JFH1+Y561F, respectively) were enhanced by the VR of JFH-1 (see polyU-J6 of each constructs in Fig. 4C) and not enhanced by the VR of J6CF (see VR-J6 of each constructs in Fig. 4C). These results indicated that the VR structure of JFH-1 was preferable for both JFH-1- and J6CF-derived NS5B and this effect was independent of the enhanced kissing-loop interaction (compare J6/N3H+3′UTR-JFH1 wt and A450S vs. Y561F in Fig. 4C).

Discussion

It has been demonstrated previously that HCV JFH-1, the only strain that replicates and produces virions efficiently in cell culture systems, expresses high replication activity without adaptive mutations [8]. We have previously reported that the N3H and N5BX regions of JFH-1 were able to rescue replication of the genotype 2a replicons [12]. The NS3 helicase and N5BX regions have been shown to be important to the virus production in HuH-7 cells. We have continued this line of experiment in the current study by focusing on RdRP activity and the genome structure in the 5BSL3.2 (CRE) to 3′X region. Following these aims, we were able to define the amino acids, nucleotides, and structural elements of JFH-1 required to confer replication competence and replication efficiency to the closely related J6CF.

In the present study, we identified five JFH-1-type amino acid residues in NS5B (Q377R, A450S, S455N, R517K, and Y561F) important for HCV replication by the *in vitro* polymerase activity assay and *in vivo* assays using replicons and full length HCV RNA. These amino acid residues are all in the thumb domain of HCV RdRP. All of these JFH-1-type substitutions increased the polymerase activity of J6CF RdRP. J6CF-type amino acids substitution into JFH-1 RdRP, including R377Q, S450A, K517R, and F561Y, reduced polymerase activity, while the N455S substitution demonstrated similar activity to the JFH-1 wt. The A450S and S455N substitutions resulted in the most significant enhancement of 1b [13] and J6CF RdRP (Fig. 1), respectively. aa 450 is located at the tip of the β-hairpin, while aa 455 is located close to the lower portions of the β-hairpin that may control the entry of the RNA template [13]. Both the β-hairpin (aa 450 to 455) and the β-strand (aa 560 to 565) of the thumb domain play an important role in RNA binding due to their extensive hydrogen-bonding network [23]. The β-hairpin has been shown to prevent the recruitment of the primer-template complex into the RNA-binding site to ensure accurate initiation from the 3′ end of the template [24,25]. A450S and S455N are thought to possibly affect J6CF RdRP structure by changing the spacing of the nucleic acid binding pocket occluded by the β-hairpin. As JFH-1 N455S did not decrease the polymerase activity of JFH-1, the thumb domain of JFH-1 may be optimized to control the position or movement of the β-hairpin. Simister *et al.* have recently reported that the higher *in vitro* polymerase activity of JFH-1 was due to a higher *de novo* initiation efficiency that may be due to a closed conformation of the JFH-1 polymerase [26]. Eight amino acid mutations in NS5B of JFH-1 are hypothesized to be responsible for the conformational differences in the NS5B sequences JFH-1 and the 2a consensus [26]. However, these amino acids did not overlap with the mutations that we identified to be important for replication. Taken together, these two studies suggested that the thumb structure surrounding the β-hairpin is important to RdRP activity [26]. We only tested six of 29 amino acid differences and other mutations are possibly important to RdRP activity. However, SKF and SNKF slightly increased replication activity compared to the replicon with entire NS5B of JFH-1 (Fig. 2C). These results suggest that there may be some JFH-1-type variants in NS5B region that inhibit the replication activity of JFH-1. The JFH-1 and J6CF 5BSL regions (Fig. S2) differ in three amino acids. The JFH-1-type substitution R517K and Y561F increased replication, while the variation at aa 571 did not affect replication. This means that there are no JFH-1 variants in 5BSL region that inhibit replication activity. However, some other mutations which were not tested outside of 5BSL region may inhibit replication. Taken together, we considered that is why the replicon with 5BSLX of JFH-1 had almost the same replication activity as the replicon with entire NS5B region of JFH-1.

After comparing the activating effects of A450S and S455N vs. R517K and Y561F in the *in vitro* polymerase, *in vivo* RNA replication and virus production assays, we hypothesized that amino acids 517 and 561 likely control HCV genome replication via interactions with additional host and viral factors, including the NS3 helicase and 3′UTR. A450S enhances polymerase activity alone, while R517K and Y561F enhance genome transcription and replication activity via additional factors. The aa 455 and 517 are known to be located at the surface of the polymerase, and these mutations may affect interactions with the proteins that play important roles in RNA replication.

The combination of A450S, R517K, and Y561F substitutions conferred replication activity to the replicon with J6CF RdRP. The results of the core production were in agreement with the results from the replicon assay and suggested that these amino acid mutations affected only RNA replication and did not affect the additional steps in the virus life cycle within the cells, such as virus particle assembly and virus secretion.

We did, however, observe a discrepancy between the effects of the mutations on *in vitro* RNA polymerase activity and *in vivo* RNA replication and virus production activities. The S455N mutation conferred the highest levels of activity on J6CF RdRP *in vitro*, while Y561F conferred the highest replication and virus production activities on J6/N3H+3′UTR-JFH1 in the cells. We did not observe any combination effects of the substitutions in the *in vitro* polymerase assays, while strong combination effects of the substitutions were observed on replication and core production *in vivo*. In addition, the combination of only three substitutions (SKF; A450S, R517K, and Y561F) was enough to increase HCV replication to levels similar to that of the construct harboring both the entire NS5B region and the 3′UTR of JFH-1. We did not observe any combination effects of the substitutions in the *in vitro* polymerase assays using 1b RdRP [13]. However, a discrepancy between polymerase activity *in vitro* and replication activity was also reported for GTP binding site mutants [27].

Discrepancies between the results from *in vitro* polymerase activity assays and *in vivo* replication assays may arise because of differences in the assay systems. In an *in vitro* polymerase assay, only enzymatic activity can be determined, while an *in vivo* assay of replication activity does not necessarily represent the only polymerase activity. Many viral and host factors may be involved in the RNA replication step in the cells. If a HCV replication assay using entirely reconstituted components were possible, we could compare the isolated effect of different polymerase variants on polymerase activity.

In addition to RdRP activity, host and viral factors, including *cis*-acting RNA structures in the 3′-genome must be considered in HCV replication in cells. In fact, we found a JFH-1-type nucleotide variant in NS5B region important to maintain the genome structure in the *in vivo* assay; this *cis*-acting factor could not have been identified using the *in vitro* polymerase assay. The SKF triple substitution contains the 561F variant that is important for enhanced kissing-loop interaction and high polymerase activity, suggesting that the effects of the SKF combination *in vivo* are rather due to the enhanced kissing-loop interaction.

We also analyzed the 5BSL3.2 and 3′XSL2 structures required for kissing-loop interactions, as aa 561 is in the loop domain of 5BSL3.2 and the activation effect of Y561F in the *in vivo* replicon assay was larger than in the *in vitro* polymerase assay. In order to test the effects of JFH-1-type variants of 5BSL3.2 on replication, we substituted the amino acids located downstream of the 5BSL3-to-3′X region (nt 9211 to 9678) from JFH-1 into the J6CF construct carrying the JFH-1-type NS3 helicase (J6/N3H+5BSLX-JFH1). The J6/N3H+5BSLX-JFH1 exhibited similar replication and virus production levels to J6/N3H+N5BX-JFH1. We initially focused on the amino acid differences between JFH-1 and J6CF in the region spanning between JFH-1 5BSL-to-3′X because this region was able to complement the entire JFH-1 NS5B-to-3′ X region. We identified three amino acid differences (517, 561, and 571) in the 5BSLX regions of JFH-1 and J6CF. We then introduced J6CF-type substitutions into the 5BSL3.2 region of JFH-1 RdRP. The J6CF-type substitution in JFH-1 5BSL3.2 region at positions 517 and 561, but not 571, resulted in a reduction in replication. These findings were consistent with the results of the *in vitro* polymerase assay. RNA polymerase activity *in vitro* was analyzed using the ΔC21-molecule (1–570) and JFH-1 RdRP that did not contain 571S demonstrated high levels of polymerase activity, indicating that 571S may not be important for

its high polymerase activity. The codon encoding aa 517 is located outside of the 5BSL3.2 region, suggesting that this mutation only affected polymerase activity. The codon encoding aa 561 and aa 571 are within the 5BSL3.2 region. The codon encoding aa 561 is located within the loop of the 5BSL3.2, while the codon encoding aa 571 is in the spacer region located between 5BSL3.2 and 5BSL3.3. The nucleotide mutations resulting the K517R and S571L aa substitutions were predicted to maintain 5BSL3.2 RNA secondary structures similar to that of JFH-1 using Mfold analysis [21].

Since there was the possibility that Y561F mutation affected both RdRP protein activity and genomic RNA structures, we tested the effect of nucleotide substitutions in the aa 561 codon on replication. The third nucleotide (9349U) contained within the codon encoding aa 561 is conserved among the different genotypes and essential for the kissing-loop interaction [16,22]. The second nucleotide (nt 9348) of JFH-1 is a U, while that of J6CF an A. The first nucleotide (nt 9347) of the codon should be either an A or a U, because these nucleotides are required to maintain the loop structure. Thus, a Phe (JFH-1), Tyr (J6CF and 1b), or Ile (9347A) may reside at position 561. As JFH-1 RdRP F561I retained identical activity levels to the wt (561F), hydrophobic amino acids appeared to be required in this position to maintain the high polymerase activity. Since the predicted secondary structures of 5BSL3.2 were identical for JFH-1 and J6CF, both Phe located at position 561 and the nucleotide sequence UUU in JFH-1 were essential for the high replication activity in cultured cells.

The conserved sequences of the kissing-loop interaction were UCACAGC (nt 9349–9355) in 5BSL3.2 and GCUGUGA (nt 9612–9618) in 3′X SL2. In the case of JFH-1, the nucleotide located at position 9348 was U and the nucleotide located at position 9619 was A, resulting in extended kissing-loop interaction sequence in JFH-1. When we introduced a mutation into the 3′X SL2 region (nt 9619) that was expected to abolish the extra base pair next to the interaction site, replication activity was significantly decreased. In addition, a combination of the F561Y and 3′X SL2m substitutions, expected to restore the extra base pair between nt 9348 and nt 9619, restored replication. Replication level of this double substitution was slightly lower than that of the wt constructs, possibly due to the preference for Phe at 561 over Tyr for genome replication. Mfold analysis also revealed that RNA secondary structure was not affected following the introduction of these substitutions. U at nucleotide position 9348 was previously identified in various HCV strains registered in GenBank [7]. Taken together, these findings suggested that the strong kissing-loop interaction of the JFH-1 genome supports efficient genome replication in HuH-7 cells. We also tested the effect of Y561F substitution in two other genotypes, H77S (GT1a) and HCV-N (GT1b). While the Y561F substitution increased replication activity in both genotype 1 strains, the Y561F effect on the genotype 1 strains was much smaller than its corresponding effect on J6CF. These results may indicate that the levels of Y561F effect for viral RNA replication are different among the genotypes. These results may also indicate that the Y561F substitution enhanced replication of strains with a substantial replication capacity. In case of J6CF, the Y561F effect was only observed with N3H region and VR of JFH-1 (Fig. 4C, compare VR-J6 and polyU-J6 of J6/N3H+3′UTR-JFH1+Y561F). This result suggested that the Y561F effect was difficult to detect with replication-incompetent clones or clones with weak replication, and also suggested that other mutations or regions are important to replicate genotype 1 replicon efficiently. Therefore, we need more efficient replicating clone of genotype 1 to determine the effect and importance of this mutation on genotype 1 strains.

We next analyzed the effects of 3′UTR structure on replication and demonstrated that the polyU/UC of JFH-1 was 27 nucleotides shorter than that of J6CF. The shorter polyU/UC and the RNA structure of the VR of JFH-1 appeared enhance efficient replication. When using the activated RdRP (SKF) and the optimal RNA structure of the 3′ genome together with the JFH-1 NS3 helicase, we found that J6CF, which did not replicate in cells, was successfully converted to a replicating virus. The VR sequence is generally not conserved, even among strains within the same genotype, and the effects of VR on HCV replication remain controversial [14,15,28]. Our data revealed that the VR of JFH-1 was more favorable than that of J6CF for replication. Substitution of the VR from JFH-1 to J6CF significantly reduced replication levels 1000-fold. This dramatic change in replication activity was likely due to alterations in the RNA structure with a mutation at nt 9458. The predicted RNA structure of the VR and replication activity of the constructs containing substitutions or mutations to the VR were completely correlated. It is therefore very likely that cellular and viral factors interact with the HCV genome in this region, and that the specific nucleotide sequence and higher structure of the VR may be essential for these interactions. There is a possibility of genetic interaction between the VR and NS5B region. These kinds of interaction may also affect on polymerase activity.

The length of the polyU/UC tract appeared to be flexible and even differed within the same genotype. Even though JFH-1 and J6CF shared an identical 3′X, the JFH-1 poly U/UC tract (nt 9483–nt 9579) was 27 U shorter than that of J6CF (nt 9483–nt 9606). Thus, we examined whether the polyU/UC tract could be exchanged between JFH-1 and J6CF. The J6/N3H+5BSLX-JFH1 variant that contained the J6CF polyU/UC exhibited a four-fold reduction in replication, demonstrating that the polyU/UC did indeed affect replication. Several published papers have investigated the affects of length on the polyU/UC region [14,15,16]. Several viral and cellular proteins have also been reported to interact with the polyU sequence [29,30,31,32,33,34,35,36]. The preferential length and nucleotide sequence of the polyU/UC may be determined by interaction with these factors.

In conclusion, we found that high RdRP activity, enhanced kissing-loop interaction between 5BSL3.2 and 3′X SL2, optimal VR structure and a shorter polyU/UC tract in JFH-1 contributed to the high levels of HCV RNA replication and virus production in cultured cells. As NS3 helicase region of JFH-1 is also important for replication and viral production of J6CF, the replication enhancing mechanism of NS3 helicase region should be analyzed.

Supporting Information

Figure S1 (A). Purified HCV J6CF and JFH-1 mutant RNA polymerases. HCV RdRp variants were purified as indicated in the Materials and Methods section. Five pmol of RdRp were applied on 10% SDS-PAGE and stained with Coomassie brilliant blue. The designations of HCV J6CF and JFH-1 wt and mutants are indicated above the PAGE. M; molecular weight marker (Takara), and the position is indicated on the left. (B). Representative PAGE of *in vitro* transcription of HCV J6CF and JFH-1 mutant RNA polymerases. *In vitro de novo* transcription was performed as indicated in the Materials and Method section. [^{32}P]-RNA products were applied on 6% PAGE containing 8 M urea. The autoradiography was analyzed by Typhoon trio plus image analyzer. The radio isotope count of 184 nt RNA product was measured and compared to that of JFH-1 RdRp wt in the same PAGE. The designations of HCV J6CF and JFH-1 wt and mutants are indicated above the PAGE. M; [^{32}P]-25 base DNA

ladder (Takara), and the position is indicated on the left. The position of 184 nt RNA product is indicated on the right.
Found at: doi:10.1371/journal.ppat.1000885.s001 (0.45 MB TIF)

Figure S2 Comparisons of the amino acid sequence of NS5B of JFH-1 and J6CF. The 5BSL region is indicated with a box.
Found at: doi:10.1371/journal.ppat.1000885.s002 (0.13 MB TIF)

Figure S3 Effect of Y561F substitution on replication activity of genotype 1 replicons. Replication activity of genotype 1a (H77S:(A)) and 1b (HCV-N:(B)) replicons. Subgenomic RNA was synthesized *in vitro* from wild-type or chimeric replicon constructs. Transcribed subgenomic RNA (5 μg) was then electroporated into HuH-7 cells and the cells serially harvested 4, 24, and 48 h after transfection. The harvested cells were lysed and the luciferase activity of the cell lysates was measured. The assays were performed three times independently, and the results expressed as luciferase activities (RLU). Luciferase activity is expressed as the change in RLU (n-fold) relative to the luciferase activity 4 h after transfection. Each value was corrected for transfection efficiency as determined by measuring the luciferase activity 4 h after transfection. Data are presented as the mean ± standard deviation for luciferase activity.

Found at: doi:10.1371/journal.ppat.1000885.s003 (0.08 MB TIF)

Table S1 Oligonucleotides used for construction.
Found at: doi:10.1371/journal.ppat.1000885.s004 (0.04 MB XLS)

Text S1 Supplementary materials and methods
Found at: doi:10.1371/journal.ppat.1000885.s005 (0.03 MB DOC)

Acknowledgments

We thank Y. Gao for her technical assistance. The pJ6CF plasmid was kindly provided by Jens Bukh. The pCVH77c plasmid was kindly provided by Robert H. Purcell. The pFKI389/neo/NS3-3′/wt plasmid was kindly provided by Ralf Bartenschlager. The pH77-S, pNNeo/3-5B, and pNNeo/3-5BΔGDD plasmids were kindly provided by Stanley M. Lemon.

Author Contributions

Conceived and designed the experiments: AM LW XT TS TK TW TT. Performed the experiments: AM LW XT. Analyzed the data: AM LW XT TS TK TW TT. Contributed reagents/materials/analysis tools: TD DA YT MM. Wrote the paper: AM LW TW TT.

References

1. Lemon S, Walker C, Alter M, Yi M (2007) Hepatitis C virus. In: Knipe D, Howley P, eds. Fields Virology 5 ed. PhiladelphiaPA: Lippincott-Raven Publishers. pp 1253–1304.
2. Wasley A, Alter MJ (2000) Epidemiology of hepatitis C: geographic differences and temporal trends. Semin Liver Dis 20: 1–16.
3. Grakoui A, Wychowski C, Lin C, Feinstone SM, Rice CM (1993) Expression and identification of hepatitis C virus polyprotein cleavage products. J Virol 67: 1385–1395.
4. Hijikata M, Mizushima H, Tanji Y, Komoda Y, Hirowatari Y, et al. (1993) Proteolytic processing and membrane association of putative nonstructural proteins of hepatitis C virus. Proc Natl Acad Sci U S A 90: 10773–10777.
5. Tsukiyama-Kohara K, Iizuka N, Kohara M, Nomoto A (1992) Internal ribosome entry site within hepatitis C virus RNA. J Virol 66: 1476–1483.
6. Tanaka T, Kato N, Cho MJ, Shimotohno K (1995) A novel sequence found at the 3′ terminus of hepatitis C virus genome. Biochem Biophys Res Commun 215: 744–749.
7. You S, Stump DD, Branch AD, Rice CM (2004) A cis-acting replication element in the sequence encoding the NS5B RNA-dependent RNA polymerase is required for hepatitis C virus RNA replication. J Virol 78: 1352–1366.
8. Wakita T, Pietschmann T, Kato T, Date T, Miyamoto M, et al. (2005) Production of infectious hepatitis C virus in tissue culture from a cloned viral genome. Nat Med 11: 791–796.
9. Zhong J, Gastaminza P, Cheng G, Kapadia S, Kato T, et al. (2005) Robust hepatitis C virus infection in vitro. Proc Natl Acad Sci U S A 102: 9294–9299.
10. Lindenbach BD, Evans MJ, Syder AJ, Wolk B, Tellinghuisen TL, et al. (2005) Complete replication of hepatitis C virus in cell culture. Science 309: 623–626.
11. Pietschmann T, Kaul A, Koutsoudakis G, Shavinskaya A, Kallis S, et al. (2006) Construction and characterization of infectious intragenotypic and intergenotypic hepatitis C virus chimeras. Proc Natl Acad Sci U S A 103: 7408–7413.
12. Murayama A, Date T, Morikawa K, Akazawa D, Miyamoto M, et al. (2007) The NS3 helicase and NS5B-to-3′X regions are important for efficient hepatitis C virus strain JFH-1 replication in Huh7 cells. J Virol 81: 8030–8040.
13. Weng L, Du J, Zhou J, Ding J, Wakita T, et al. (2009) Modification of hepatitis C virus 1b RNA polymerase to make a highly active JFH1-type polymerase by mutation of the thumb domain. Arch Virol 154: 765–773.
14. Friebe P, Bartenschlager R (2002) Genetic analysis of sequences in the 3′ nontranslated region of hepatitis C virus that are important for RNA replication. J Virol 76: 5326–5338.
15. Yanagi M, Purcell RH, Emerson SU, Bukh J (1999) Hepatitis C virus: an infectious molecular clone of a second major genotype (2a) and lack of viability of intertypic 1a and 2a chimeras. Virology 262: 250–263.
16. You S, Rice CM (2008) 3′ RNA elements in hepatitis C virus replication: kissing partners and long poly(U). J Virol 82: 184–195.
17. Nakabayashi H, Taketa K, Miyano K, Yamane T, Sato J (1982) Growth of human hepatoma cells lines with differentiated functions in chemically defined medium. Cancer Res 42: 3858–3863.
18. Kuiken C, Combet C, Bukh J, Shin IT, Deleage G, et al. (2006) A comprehensive system for consistent numbering of HCV sequences, proteins and epitopes. Hepatology 44: 1355–1361.
19. van den Hoff MJ, Moorman AF, Lamers WH (1992) Electroporation in 'intracellular' buffer increases cell survival. Nucleic Acids Res 20: 2902.
20. Kato T, Date T, Miyamoto M, Sugiyama M, Tanaka Y, et al. (2005) Detection of anti-hepatitis C virus effects of interferon and ribavirin by a sensitive replicon system. J Clin Microbiol 43: 5679–5684.
21. Zuker M (2003) Mfold web server for nucleic acid folding and hybridization prediction. Nucleic Acids Res 31: 3406–3415.
22. Friebe P, Boudet J, Simorre JP, Bartenschlager R (2005) Kissing-loop interaction in the 3′ end of the hepatitis C virus genome essential for RNA replication. J Virol 79: 380–392.
23. Leveque VJ, Johnson RB, Parsons S, Ren J, Xie C, et al. (2003) Identification of a C-terminal regulatory motif in hepatitis C virus RNA-dependent RNA polymerase: structural and biochemical analysis. J Virol 77: 9020–9028.
24. Zhong W, Ferrari E, Lesburg CA, Maag D, Ghosh SK, et al. (2000) Template/primer requirements and single nucleotide incorporation by hepatitis C virus nonstructural protein 5B polymerase. J Virol 74: 9134–9143.
25. Hong Z, Cameron CE, Walker MP, Castro C, Yao N, et al. (2001) A novel mechanism to ensure terminal initiation by hepatitis C virus NS5B polymerase. Virology 285: 6–11.
26. Simister P, Schmitt M, Geitmann M, Wicht O, Danielson UH, et al. (2009) Structural and functional analysis of hepatitis C virus strain JFH1 polymerase. J Virol.
27. Cai Z, Yi M, Zhang C, Luo G (2005) Mutagenesis analysis of the rGTP-specific binding site of hepatitis C virus RNA-dependent RNA polymerase. J Virol 79: 11607–11617.
28. Arumugaswami V, Remenyi R, Kanagavel V, Sue EY, Ngoc Ho T, et al. (2008) High-resolution functional profiling of hepatitis C virus genome. PLoS Pathog 4: e1000182. doi:10.1371/journal.ppat.1000182.
29. Kanai A, Tanabe K, Kohara M (1995) Poly(U) binding activity of hepatitis C virus NS3 protein, a putative RNA helicase. FEBS Lett 376: 221–224.
30. Luo G, Hamatake RK, Mathis DM, Racela J, Rigat KL, et al. (2000) De novo initiation of RNA synthesis by the RNA-dependent RNA polymerase (NS5B) of hepatitis C virus. J Virol 74: 851–863.
31. Huang L, Hwang J, Sharma SD, Hargittai MR, Chen Y, et al. (2005) Hepatitis C virus nonstructural protein 5A (NS5A) is an RNA-binding protein. J Biol Chem 280: 36417–36428.
32. Gontarek RR, Gutshall LL, Herold KM, Tsai J, Sathe GM, et al. (1999) hnRNP C and polypyrimidine tract-binding protein specifically interact with the pyrimidine-rich region within the 3′NTR of the HCV RNA genome. Nucleic Acids Res 27: 1457–1463.
33. Luo G (1999) Cellular proteins bind to the poly(U) tract of the 3′ untranslated region of hepatitis C virus RNA genome. Virology 256: 105–118.
34. Petrik J, Parker H, Alexander GJ (1999) Human hepatic glyceraldehyde-3-phosphate dehydrogenase binds to the poly(U) tract of the 3′ non-coding region of hepatitis C virus genomic RNA. J Gen Virol 80 (Pt12): 3109–3113.
35. Spangberg K, Wiklund L, Schwartz S (2001) Binding of the La autoantigen to the hepatitis C virus 3′ untranslated region protects the RNA from rapid degradation in vitro. J Gen Virol 82: 113–120.
36. Spangberg K, Wiklund L, Schwartz S (2000) HuR, a protein implicated in oncogene and growth factor mRNA decay, binds to the 3′ ends of hepatitis C virus RNA of both polarities. Virology 274: 378–390.

Biochemical and Biophysical Research Communications 395 (2010) 565–571

Contents lists available at ScienceDirect

Biochemical and Biophysical Research Communications

journal homepage: www.elsevier.com/locate/ybbrc

Biological properties of purified recombinant HCV particles with an epitope-tagged envelope

Hitoshi Takahashi [a,b], Daisuke Akazawa [a,b], Takanobu Kato [a], Tomoko Date [a], Masayuki Shirakura [a,b], Noriko Nakamura [b], Hidenori Mochizuki [b], Keiko Tanaka-Kaneko [c], Tetsutaro Sata [c], Yasuhito Tanaka [d], Masashi Mizokami [e], Tetsuro Suzuki [a], Takaji Wakita [a,*]

[a] Department of Virology II, National Institute of Infectious Diseases, Tokyo, Japan
[b] Toray Industries, Inc., Kanagawa, Japan
[c] Department of Pathology, National Institute of Infectious Diseases, Tokyo, Japan
[d] Department of Clinical Molecular Informative Medicine, Nagoya City University Graduate School of Medicine, Nagoya, Japan
[e] Research Center for Hepatitis & Immunology, Kohnodai Hospital, International Medical Center of Japan, Chiba, Japan

ARTICLE INFO

Article history:
Received 3 April 2010
Available online 23 April 2010

Keywords:
Hepatitis C virus
Envelope protein
Purification
Particle
Vaccine

ABSTRACT

To establish a simple system for purification of recombinant infectious hepatitis C virus (HCV) particles, we designed a chimeric J6/JFH-1 virus with a FLAG (FL)-epitope-tagged sequence at the N-terminal region of the E2 hypervariable region-1 (HVR1) gene (J6/JFH-1/1FL). We found that introduction of an adaptive mutation at the potential *N*-glycosylation site (E2N151K) leads to efficient production of the chimeric virus. This finding suggests the involvement of glycosylation at Asn within the envelope protein(s) in HCV morphogenesis.

To further analyze the biological properties of the purified recombinant HCV particles, we developed a strategy for large-scale production and purification of recombinant J6/JFH-1/1FL/E2N151K. Infectious particles were purified from the culture medium of J6/JFH-1/1FL/E2N151K-infected Huh-7 cells using anti-FLAG affinity chromatography in combination with ultrafiltration. Electron microscopy of the purified particles using negative staining showed spherical particle structures with a diameter of 40–60 nm and spike-like projections. Purified HCV particle-immunization induced both an anti-E2 and an anti-FLAG antibody response in immunized mice. This strategy may contribute to future detailed analysis of HCV particle structure and to HCV vaccine development.

1. Introduction

The hepatitis C virus (HCV) causes chronic hepatitis, liver cirrhosis and hepatocellular carcinoma [1]. HCV is a positive strand RNA virus belonging to the *Hepacivirus* genus in the Flaviviridae family. The HCV genome consists of about 9600 nucleotides and contains three regions: a 5′ non-coding region of 341 nucleotides containing the sequence for the IRES structure, a coding region of about 9000 nucleotides, which encodes about 10 viral proteins, and a 3′ non-coding region of about 200 nucleotides depending on the size of the poly-uridylate track within this region [2,3].

The main therapy for HCV is treatment with pegylated-interferon and rivabirin. However, these agents show little effect in patients that have a high titer of HCV RNA, genotype 1. Thus, it is necessary to develop new, more effective therapies and preventive treatments to counteract HCV infection. As yet, no preventive vaccine is available for HCV. A recombinant HCV vaccine based on the viral envelope protein E1/E2 has been reported that generated neutralizing antibodies (nAb) in animals [4]. These nAbs were capable of limiting HCV pseudoparticles (HCVpp) and HCV cell culture (HCVcc) infection.

Recently, a genotype 2a strain of HCV named JFH-1 was discovered. This strain can efficiently replicate in the Huh-7 cell line [5], and an *in vitro* culture system of infectious HCV has also been successfully developed using the JFH-1 genome [6–8]. The JFH-1 viral production system is expected to become a powerful tool for HCV vaccine development. In this study, we developed a simple strategy for purification of recombinant HCV particles from the media of infected Huh-7 cells for structural analysis and for vaccine development using the JFH-1 genome.

2. Materials and methods

2.1. Plasmids

Plasmid pJ6/JFH-1 was generated from pJFH-1 by replacement of the 5′ untranslated region with the p7 region of J6 [9]. The

* Corresponding author. Address: Department of Virology II, National Institute of Infectious Diseases, 1-23-1 Toyama, Shinjuku, Tokyo 162-8640, Japan. Fax: +81 3 5285 1161.
E-mail address: wakita@nih.go.jp (T. Wakita).

0006-291X/$ - see front matter © 2010 Elsevier Inc. All rights reserved.
doi:10.1016/j.bbrc.2010.04.081

plasmids pJ6/JFH-1/1FL and pJ6/JFH-1/3FL were constructed by introduction of a single (DYKDDDDKGGG) or triple (DYKDHDG-DYKDHDIDYKDDDDKGGG) FLAG-tag sequence, respectively, into pJ6/JFH-1, which replaced part of the E2 HVR1 (amino acids 394–400) region. These two plasmids were then modified by introduction of a Lys residue to replace the Asn at amino acid position 151 of the E2 sequence, creating pJ6/JFH-1/1FL/E2N151K and pJ6/JFH-1/3FL/E2N151K, respectively.

The J6E2 gene (codons 1490–2500) was generated by PCR amplification from pJ6CF. The sense and antisense primers used were: 5′-CACAAGCTTCGCACCCATACTGTTGGGG-3′ and 5′-ACAGGATCCCAT-CGGACGATGTATTTTGTG-3′, respectively. For cloning purposes, HindIII or BamHI sites (underlined) were added to the primers. The amplified DNA was digested and inserted into p3XFLAG-CMV-13 (SIGMA, Saint Louis, MO).

The plasmid CDM-J6E2Fc encodes the J6E2 sequence downstream of the preprotrypsin leader sequence. pCDM-J6E2Fc was digested with SacI and BamHI, and the DNA fragment containing the preprotrypsin leader and J6E2 sequence was inserted into pCD4Rg (a kind gift from Dr. Brian Seed, Harvard Medical School) from which the SacI–BamHI fragment containing the CD4 gene was removed. This ligation resulted in the creation of a plasmid encoding a fusion gene of E2 and human IgG1-Fc.

2.2. Cell culture

The human hepatoma cell line, Huh-7, was maintained in DMEM supplemented with 10% FBS at 37 °C in a 5% CO_2 incubator.

2.3. In vitro synthesis of HCV RNA and RNA transfection of Huh cells

HCV RNA was synthesized from the plasmids described above *in vitro* using a MEGAscript T7 kit (Ambion, Austin, TX). Synthesized HCV RNA was then electroporated into cells as previously described [10]. The transfected cells were transferred onto 100-mm culture dishes containing culture medium.

2.4. Quantification of HCV core protein and RNA

The HCV core protein in cell culture supernatants or in purified HCV samples was quantified by enzyme immunoassay using a HCV core ELISA kit (Ortho Clinical Diagnostics). HCV RNA in purified HCV samples was quantified by RTD-PCR as previously described [11].

2.5. Deglycosylation with PNGase F

For deglycosylation reactions, the Enzymatic In-Solution N-Deglycosylation kit (Sigma) was used according to the manufacturer's instructions. Briefly, lysates of passaged cells were incubated for 10 min at 100 °C in denaturation buffer and then in the presence of PNGase F enzyme for 1 h at 37 °C. These samples were analyzed by Western blotting as described below using anti-FLAG (SIGMA) and anti-GAPDH (CHEMICON, Temecula, CA) antibodies.

2.6. Sequence analysis

The cDNAs of the HCV genome were synthesized from total RNA isolated from HCV RNA-transfected cells [5]. These cDNA were subsequently amplified using DNA polymerase (*TaKaRa LA Taq*, Takara, Shiga, Japan). The sequence of the amplified DNA was determined by the 3130 Genetic Analyzer (Applied Biosystems, Foster city, CA).

2.7. Purification of recombinant HCV particles

Culture supernatants from Huh-7 cells transfected with FLAG-tagged HCV RNA were harvested. The medium was concentrated by ultrafiltration using the pellicon-2 300 system (Millipore, Bedford, MA) and was subjected to affinity chromatography using an Anti-FLAG M2 affinity gel (Sigma). Virus particles were eluted using the 3×FLAG Peptide (Sigma) and were concentrated by ultracentrifugation for 2 h at 50,000 rpm at 4 °C.

2.8. Determination of the viral infectious titer

The infectious titer was determined by the method as previously described and was expressed as the number of focus-forming units per milliliter (FFU/mL) [6].

2.9. Western blotting

The purified HCV sample was lysed using a buffer containing 0.1 M Tris–HCl (pH 6.8), 4% SDS, 1.2% 2-mercaptoethanol, 20% glycerol, and Bromophenol blue. SDS–PAGE and immunoblotting were performed as previously described [6]. Antibodies used for immunoblotting were: anti-HCV core (clone 2H9) [6], anti-E1 (B7567) [6], and anti-E2 (clone 8D10-3, unpublished).

2.10. Electron microscopy

Concentrated, purified HCV particles were allowed to settle on carbon-coated copper grids and were stained with 4% uranylacetate. The grids were examined in a transmission electron microscope (H-7650, Hitachi, Tokyo, Japan) and were photographed at an instrumental magnification of 50,000×.

2.11. Sucrose density gradient analysis

The purified HCV sample containing 266 fmol of the HCV core was layered on a stepwise sucrose gradient (10–60%, wt/vol) and was centrifuged for 16 h in an SW41 rotor (Beckman Coulter, Fullerton, CA) at 35,000 rpm at 4 °C. After centrifugation, 12 fractions were harvested from the bottoms of the tubes. For each fraction, the core protein concentration was determined using an immunoassay. The HCV RNA titer was determined using RTD-PCR. The infectious titer was determined using an immunofluorescence assay as described above.

2.12. HCV particle-immunization

The purified HCV particles described above were inactivated by UV-irradiation, and 2 pmol of the HCV core protein of the particles were intraperitoneally injected into 4 week old BALB/c female mice ($n = 3$). Immunization was repeated four times at 2-week intervals (0, 2, 4 and 6 weeks). The Sigma Adjuvant System (Sigma), composed of monophosphoryl lipid A and trehalose dicorynomycolate, was used as an adjuvant. Saline alone was injected into control mice. Sera were collected at 1, 3, 5 and 7 weeks after immunization.

2.13. EIA for measurement of anti-E2 and anti-FLAG antibody responses

Recombinant J6E2/Fc or the FLAG peptide antigen (Sigma) was bound to microtiter plates (Nunc, Rochester, NY, USA) overnight at 4 °C, at a concentration of 50 ng per well. Recombinant J6E2/Fc was produced from COS-1 cells transfected with the CDM-J6E2Fc plasmid, which encodes the J6CF-E2 region (aa 384–720) fused with the Fc region of human IgG. The plates were blocked with Blocking One solution (Nacalai Tesque, Kyoto, Japan) and were washed with PBS containing 0.05% Tween 20 (washing buffer). Serum samples were diluted in washing buffer and were transferred to the blocked, antigen coated plates. After a 1.5-h incubation,

the plates were washed and bound antibody was detected using an HRP-conjugated anti-mouse antibody (GE healthcare, Buckinghamshire, England) and 3,3′,5,5′-tetramethylbenzidine (TMBZ) as a substrate (Sumitomo Bakelite, Tokyo, Japan).

3. Results

3.1. Production of recombinant HCV with an epitope-tagged envelope

To facilitate purification of recombinant HCV particles secreted into the culture medium of transfected cells, we constructed recombinant HCV with a FLAG-epitope-tagged envelope, which could then be purified by affinity chromatography using an anti-FLAG-agarose column. The FLAG-tagged HCV genome J6/JFH-1/3FL with the J6CF structural region was constructed by introducing a triple FLAG-tag sequence into the HVR1 of E2 (Fig. 1A). This region was selected for epitope-tag insertion because we predicted that this region would lie on the outside of the virus particles and would be tolerant to amino acid changes. Recombinant HCV particles were produced following transfection of Huh-7 cells with viral RNA, and were secreted into the culture medium.

RNA-transfected cells were passaged every 4 or 5 days. The level of the HCV core protein in the culture supernatant was measured over a period of 70 days (Fig. 1B). In contrast to the gradually increasing level of the core protein in J6/JFH-1 cells over time, the level of the core protein in the supernatants of the J6/JFH-1/3FL RNA-transfected cells decreased over the first 3 weeks post-transfection. Subsequently, the level began to increase and this level became equal to that of the wild-type J6/JFH-1 RNA-transfected cells 35 days post-transfection. This result suggested that after the first 35 days of culture, some mutations were introduced into the HCV genome that conferred efficient virus production during genome replication and/or that the transfected cells were altered in some way that was more favorable for viral production.

3.2. An N151K mutation facilitates the production of FLAG-tagged HCV

To determine if any adaptive mutations had arisen in the viral genome, we sequenced the full length of the HCV genome on days 8 and 35 post-J6/JFH-1/3FL RNA transfection. On day 8 post-transfection, no non-synonymous mutations were detected. However, on day 35, we found a single amino acid mutation at a potential

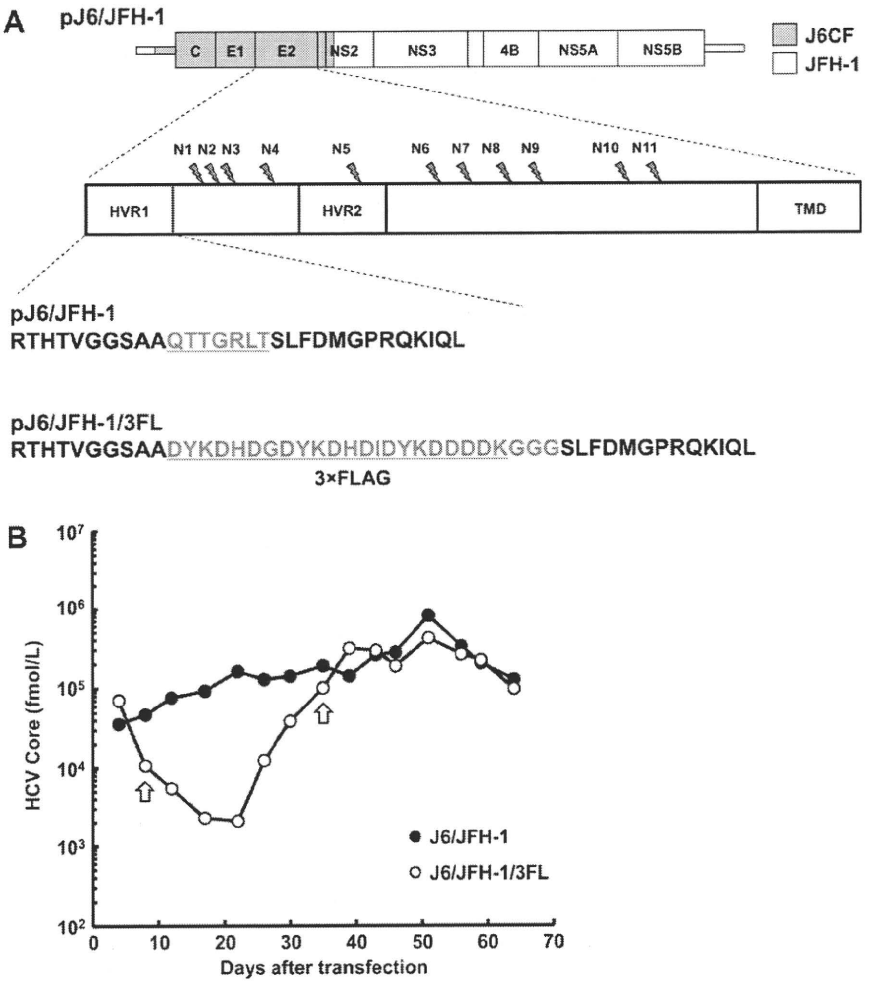

Fig. 1. Time course of HCV core protein secretion in recombinant HCV RNA-transfected cells. (A) Organization of the recombinant HCV construct pJ6/JFH-1/3FL. Open reading frames (thick boxes) are flanked by 5′- and 3′-UTRs (thin boxes). Gray, J6CF; white, JFH-1; HVR, hyper variable region; TMD, transmembrane domain. *N*-Glycosylation sites are indicated by pointers and are numbered N1–N11. The region of pJ6/JFH-1 that is replaced by the 3×FLAG sequence to generate pJ6/JFH-1/3FL is indicated at bottom. (B) HCV core protein secretion into the culture medium after HCV RNA transfection of Huh-7 cells. The HCV core protein was analyzed using an ELISA. Arrows indicate the times at which the J6/JFH-1/3FL HCV genome transfected into HCV RNA-transfected cells was sequenced.

N-glycosylation site of the E2 protein (Fig. 2A) in which asparagine at amino acid position 151 in the E2 protein was changed to lysine (E2N151K). Interestingly, this mutation was identical to that described by Delgrange et al. [12] as a mutation that was important for efficient production of HCV JFH-1. We performed Western blot analysis of cell lysates of transfected cells of different passages, using the anti-FLAG antibody as a probe for E2, to confirm that the N151K mutation abolishes one specific *N*-glycosylation. Indeed, the size of the FLAG-E2 protein was smaller on days 30 and 43 compared to that on day 4 (Fig. 2B). In contrast, the size of FLAG-E2 proteins that were deglycosylated using PNGase F was similar for all of the tested samples (Fig. 2B). This result suggested that the E2N151K mutation abolished *N*-glycosylation at this residue.

To investigate if the E2N151K mutation enhances production of FLAG-tagged HCV, we introduced the E2N151K mutation into the J6/JFH-1/3FL genome (J6/JFH-1/3FL/E2N151K). J6/JFH-1/3FL/E2N151K RNA-transfected cells were then passaged every 4 or 5 days and the level of the HCV core protein in the culture supernatant was measured over a period of 16 days (Fig. 2C). The result clearly showed that the E2N151K mutation contributes to efficient production of FLAG-tagged HCV particles.

We further analyzed the effect of the E2N151K mutation on specific viral infectivity (Table 1). The culture supernatant on day 3 post-transfection of recombinant viral RNA was therefore concentrated by ultrafiltration and tested in an infectious assay. The recombinant virus with the E2N151K mutation exhibited higher specific infectivity than the virus without this mutation. These data suggest that efficient production of infectious particles is impaired by the introduction of a FLAG-tag into the E2 protein but that this deficiency could be compensated for by the introduction of the E2N151K mutation which modifies an *N*-glycosylation site.

3.3. Purification of FLAG-tagged HCV

To purify FLAG-tagged HCV particles, we used a viral construct with a single FLAG-tag, J6/JFH-1/1FL/E2N151K (Fig. 1A), which as efficient in virus production as J6/JFH-1/3FL/E2N151K (data not shown). A total of 10 L of the culture supernatant of Huh-7 cells infected with J6/JFH-1/1FL/E2N151K was collected. This culture medium was concentrated to 300 mL by ultrafiltration and was then subjected to affinity chromatography using an anti-FLAG-agarose column. Bound virus particles were eluted using 10 mL of a

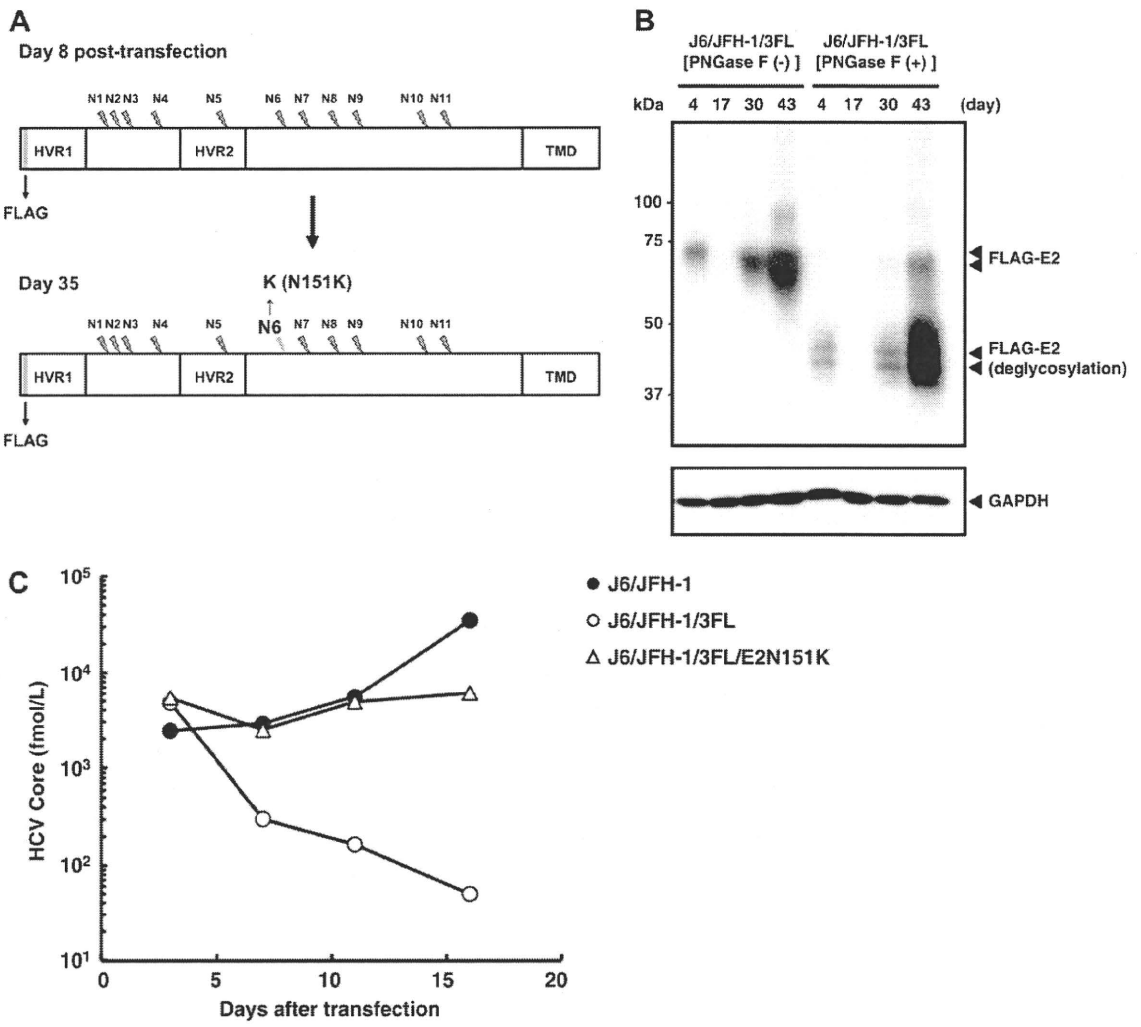

Fig. 2. Characterization of the recombinant HCV genome with an introduced N151K mutation. (A) Schematic diagram of the sequence of the E2 in the J6/JFH-1/3FL HCV RNA-transfected cells on day 8 and day 35 post-transfection. N151K replaces an Asn residue with a Lys residue at the N6 glycosylation site of E2. (B) Western blot analysis of the FLAG-E2 protein in lysates of cells transfected with J6/JFH-1/3FL RNA. Arrowheads indicate intact, and deglycosylated (PNGase F (+)), FLAG-E2 protein (upper panel) and control GAPDH protein (lower panel). (C) HCV core protein secretion into the culture medium following transfection of Huh-7 cells with HCV RNA with or without an introduced N151K mutation.

Table 1
Infectivity of recombinant viruses with or without N151K mutation.

Recombinant virus	Infectious titer ($\times 10^2$ FFU/mL)	HCV core protein ($\times 10^2$ fmol/mL)	Specific infectivity (FFU/HCV core)
J6/JFH-1/3FL	<1.7	1.6	<1.1
J6/JFH-1/3FL/E2N151K	8.3	2.0	4.2

FLAG peptide solution. Finally, the purified HCV particles were concentrated by ultracentrifugation.

The HCV yield and the amount of total protein after each purification step are summarized in Table 2. This purification process resulted in a 5000-fold concentration of the culture supernatant. The recovery of the HCV core protein in the final purified virus preparation was approximately 5%, and the virus purity was increased about 9000-fold compared to its purity in the initial culture medium. Specific infectivity was increased about 4-fold after the final step.

HCV structural proteins in the purified virus sample were examined by Western blotting (Fig. 3A). Core, E1 and E2 proteins were all detected in the purified virus preparation. Interestingly, incorporation of the E2 protein into the purified virus appeared to increase compared to incorporation of the core and E1 proteins. However, this higher apparent incorporation of FLAG-E2, may reflect the presence of free, non-virus incorporated FLAG-E2 proteins that co-purified with the FLAG-tagged virus. We further analyzed the virus particles in the purified preparation by electron microscopy (Fig. 3B–D). Substantial debris was found in the culture

Table 2
HCV yield and properties of purified recombinant HCV after each purification step.

Purification step	Volume (mL)	HCV core protein ($\times 10^2$ fmol/mL)	HCV RNA ($\times 10^7$ copies/mL)	Total protein (μg/mL)	Recovery[a] (%)	Purity[b]	Infectivity ($\times 10^2$ FFU/mL)	Specific infectivity (FFU/HCV core)
Culture supernatant	10,000	1.4	3.5	877	100	1	25	18
Concentrate (after Ultrafiltration)	300	45	57	19,597	96	0.73	743	17
Affinity purification (after Elution)	10	98	324	171	7	469	4240	43
Concentrate (after Ultracentrifugation)	0.2	1440	3220	84	5	9546	94,600	66

[a] Recovery of HCV core protein.
[b] The degree of virus purity was calculated by HCV RNA contents per μg total proteins.

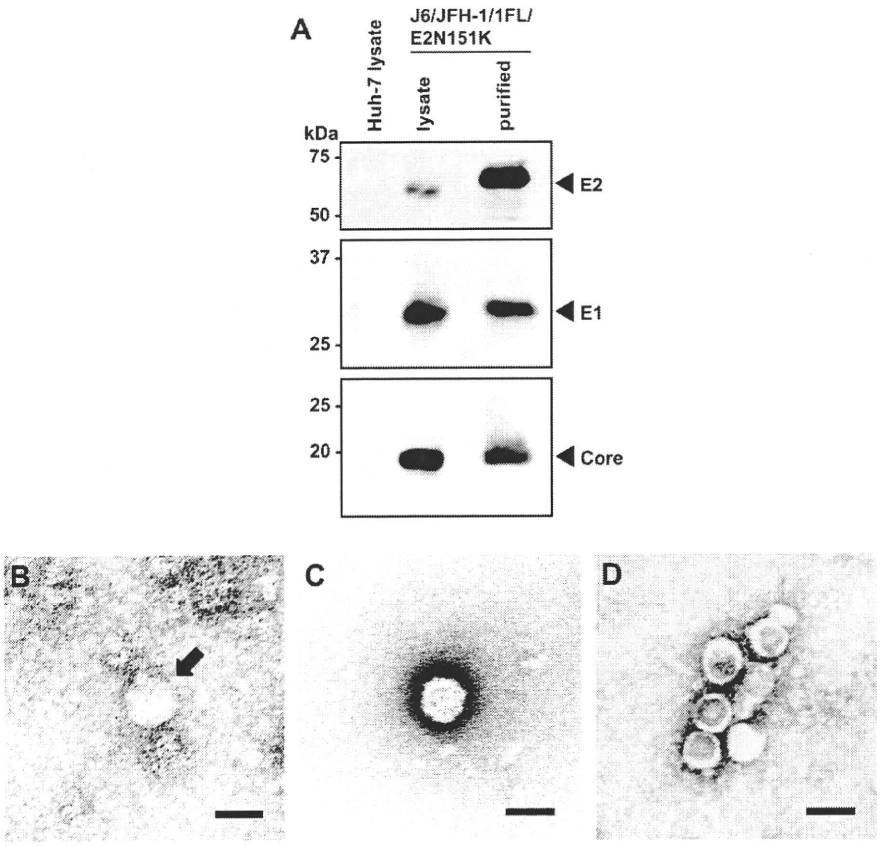

Fig. 3. Analysis of purified HCV particles. (A) Western blot analysis of viral proteins in lysates of, and in HCV particles purified from, whole-cell extracts of Huh-7 cells transfected with J6/JFH-1/1FL N151K RNA. Lysates of non-transfected cells were also analyzed. The arrowheads indicate the positions of the HCV core, E1 and E2 proteins. Marker proteins are shown at left. (B–D) Electron micrographs using negative staining of: (B) An HCV particle from culture media (indicated by an arrow.), (C) A purified HCV particle and (D) Purified HCV particles aggregated by an anti-FLAG antibody. Scale bar, 50 nm.

supernatant concentrated by ultrafiltration, which made it difficult to identify virus particles (Fig. 3B). In contrast, spherical particle structures of 40–60 nm could be clearly observed in the purified samples (Fig. 3C and D). Furthermore, the purified FLAG-tagged HCV particles were aggregated by the anti-FLAG antibody (Fig. 3D). The size and morphology of the FLAG-tagged particles were similar to each other but with slight deviations. The combined data suggest that the FLAG-tagged HCV particles can be purified by affinity chromatography using anti-FLAG-agarose.

3.4. Physical properties of purified FLAG-tagged HCV

We next further analyzed the properties of the purified FLAG-tagged HCV particles. The total number of proteins in the purified viral sample, as judged by SDS–PAGE and silver staining analysis, was much lower than that in the original culture medium (Fig. 4A). We confirmed by mass spectrometry analysis that these extra protein bands in the purified preparation were not viral proteins but were host proteins that bound to the FLAG-agarose (data not shown).

We further analyzed the purified FLAG-tagged HCV particles using a sucrose density gradient (Fig 4B). Purified virus was layered on top of a preformed continuous 10–60% sucrose gradient and was then centrifuged. Twelve fractions were collected and the HCV core protein, RNA and viral infectivity were determined for each fraction. The HCV particles migrated at a density between 1.13 and 1.16 g sucrose/mL. The density at which the peak of the HCV core protein was observed was almost identical to the density at which the HCV RNA and infectivity were detected.

3.5. Immunogenicity of purified HCV particles

To examine the immunogenicity of the FLAG-tagged HCV particles, they were injected into BALB/c mice and the sera of these mice were then analyzed for reactivity with recombinant J6E2/Fc or the FLAG peptide using an ELISA. The HCV particles were inactivated by UV-irradiation prior to injection using the Sigma Adjuvant System as an adjuvant. Both anti-E2 and anti-FLAG antibodies were induced in mice sera after four immunizations (Fig. 4C). These results suggested that the envelope proteins of the FLAG-tagged HCV

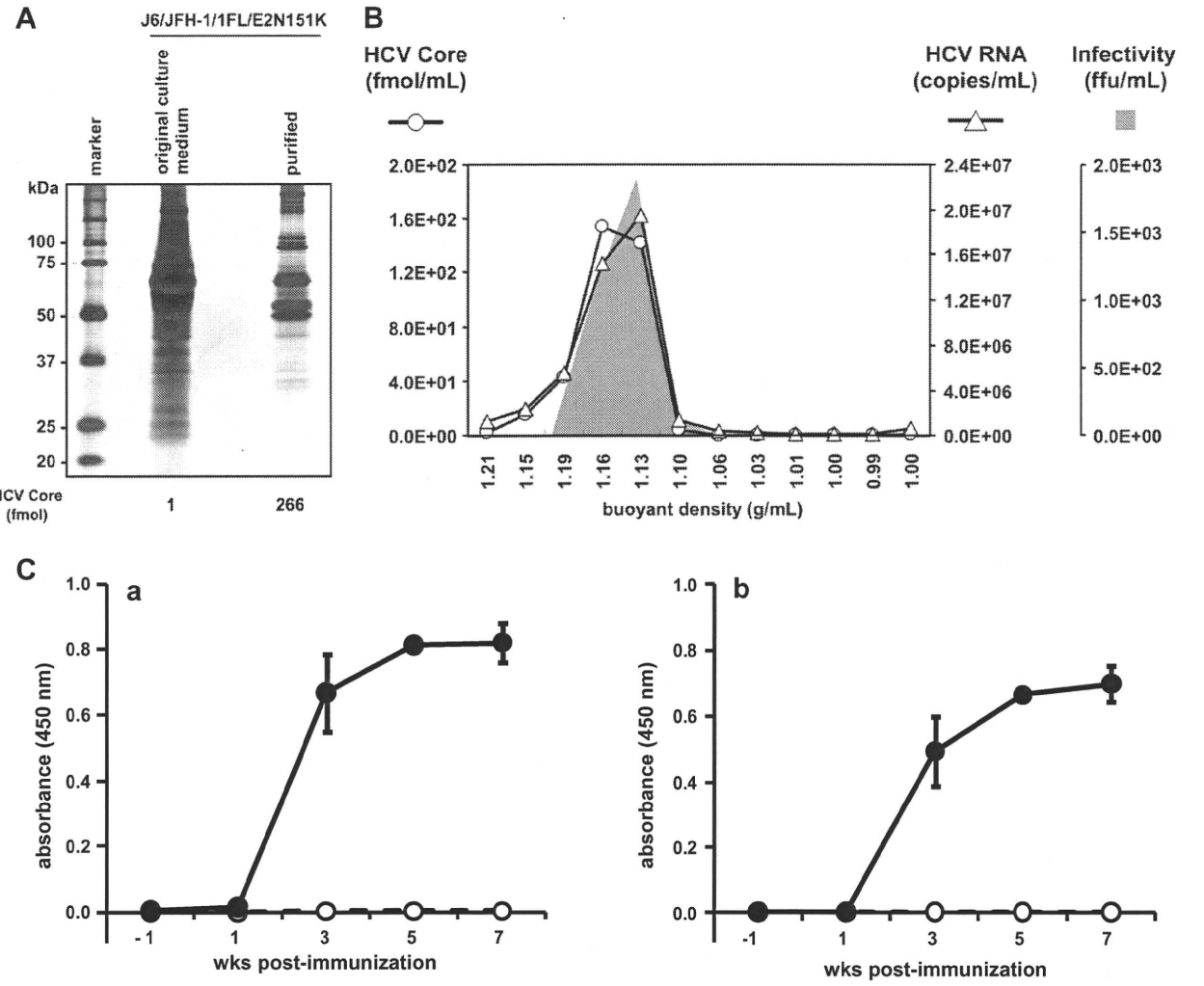

Fig. 4. Physical properties and immunogenicity of purified HCV particles. (A) Silver staining of non-purified (original culture medium) and purified HCV samples. The non-purified and purified samples contained 1 and 266 fmol, respectively, of the HCV core. (B) Sucrose density gradient analysis of purified HCV particles. The level of the HCV core protein (open circles), HCV RNA (open triangles) and the HCV infectivity towards naïve Huh-7 cells (shown in gray) were analyzed for each fraction as described in Section 2. (C) Purified HCV particles (closed circles) or saline (open circles) were intraperitoneally injected into BALB/c mice ($n = 3$), and sera were collected at the indicated times. The collected sera were examined for the presence of anti-E2 (a) and anti-FLAG (b) antibodies using the J6E2/Fc protein and the FLAG peptide as antigens in an EIA as described in Section 2.